

ANALYSIS OF VIX-LINKED FEE INCENTIVES IN VARIABLE ANNUITIES VIA CONTINUOUS-TIME MARKOV CHAIN APPROXIMATION

ANNE MACKAY^{*†}, MARIE-CLAUDE VACHON[‡] AND ZHENYU CUI[§]

[†]*Université de Sherbrooke, Sherbrooke, Québec, Canada*

[‡]*Université du Québec à Montréal, Montréal, Québec, Canada*

[§]*Stevens Institute of Technology, Hoboken, NJ 07030, USA*

ABSTRACT. We consider the pricing of variable annuities (VAs) with general fee structures under popular stochastic volatility models such as Heston, Hull-White, Scott, α -Hypergeometric, 3/2, and 4/2 models. In particular, we analyze the impact of different VIX-linked fee structures on the optimal surrender strategy of a VA contract with guaranteed minimum maturity benefit (GMMB). Under the assumption that the VA contract can be surrendered before maturity, the pricing of a VA contract corresponds to an optimal stopping problem with an unbounded, time-dependent, and discontinuous payoff function. We develop efficient algorithms for the pricing of VA contracts using a two-layer continuous-time Markov chain approximation for the fund value process. When the contract is kept until maturity and under a general fee structure, we show that the value of the contract can be approximated by a closed-form matrix expression. We also provide a quick and simple way to determine the value of early surrenders via a recursive algorithm and give an easy procedure to approximate the optimal surrender surface. We show numerically that the optimal surrender strategy is more robust to changes in the volatility of the account value when the fee is linked to the VIX index.

Keywords: Variable annuities, optimal stopping, American options, stochastic volatility, Heston model, continuous-time Markov chain

JEL Classifications: C63, G22

Date: August 1, 2022.

**Corresponding author. Email:* Anne.MacKay@USherbrooke.ca

1. INTRODUCTION

A variable annuity (or segregated fund in Canada) is a hybrid investment vehicle mainly used for retirement planning, which offers a life insurance benefit and a financial guarantee. It allows the policyholder to profit from potential gains resulting from an investment in financial markets, while offering a downside protection against losses. The real options embedded in these products are comparable to exotic options, with the following differences: the benefit may depend on the policyholder's life (survival or death), they are long-term investments (generally between 5 and 15 years, or more), and the financial guarantee is funded via a periodic fee (typically set as a percentage of the fund value) as opposed to a premium paid upfront. Different types of protection riders are offered, such as Guaranteed Minimum Maturity Benefit (GMMB), Guaranteed Minimum Death Benefit (GMDB), and Guaranteed Minimum Withdraw Benefit (GMWB); see [39] or [8] for details¹. This paper focuses on the GMMB rider, which guarantees the policyholder a minimum amount at the contract's maturity. Considering the significant size of the variable annuity market², the management of the risk associated with the guarantees embedded in variable annuities is a major concern for insurance companies, see [67]. Indeed, variable annuities guarantees entail significant risks given their long-term structure and sensitivity to various financial and demographic risks as well as to policyholders' behaviour. For the GMMB rider, this last risk is mostly due to early surrenders.

Surrender risk refers to the uncertainty facing the insurer when a policyholder has the possibility to terminate her contract before its maturity. When she does so, she is entitled to the value accumulated in the variable annuity investment account, subject to a penalty. [49] show that unexpected lapses can represent a significant risk for insurers. For this reason, surrender risk has raised special attention in the literature ([67], Chapter 18). [4] provide a universal pricing framework for various riders and considers different types of surrender behaviours: static, i.e. the contract is never surrendered; or mixed, i.e. the policyholder acts rationally and surrenders the policy as soon as it is optimal from a risk-neutral valuation perspective. Pricing variable annuities under rational surrender behaviour is equivalent to solving an optimal stopping problem and corresponds to the worst-case scenarios for insurers, in the sense that it maximizes the risk-neutral value of the contract from the policyholders' perspective. Under this assumption, [38] study the valuation of interest rate guarantees by assuming that the surrender value will be the same as the benefit value. [65] assume that the policyholder will only get a certain percentage of the fund upon surrender; this hypothesis is more in line with policies seen in practice. Under this assumption, they provide a closed-form analytical solution to the price of a GMDB with surrender in the Black-Scholes framework. In particular, they study the interaction between the surrender charges, the fee rates, and the optimal surrender level. [11] study a problem similar to the one of [65], but focus on a GMMB rather than a GMDB. It is well-known that American options with finite maturity generally do not have closed-form solutions. Thus, [11] used arbitrage-free techniques in the same vein as [47] and [17] in the context of American call and put options to derive an analytical expression for the value of the right to surrender, which is analogous to the early exercise premium in American option terminology. In particular, they study the impact of different risk factors influencing the optimal surrender boundary. In that context, [10] provide a sufficient condition on surrender charges and fees which eliminate surrender incentives for a financially rational policyholder. Recently, [46] extended the framework of [11] by analyzing how the optimal surrender boundary is affected by changes in different risk factors in a stochastic interest rate and volatility model of the Heston-Hull-White type, whereas [2] incorporate taxes into their analysis.

¹There are no consensus among practitioners and scientists for these products' name, and thus, different authors may use different terminologies for the same product.

²In United-States, the total variable annuity sales were \$125 billion in 2021, representing an increase of 25% with respect to the total VA sales in 2020. Source: LIMRA Secure Retirement Institute, U.S. Individual Annuities survey <https://www.limra.com/siteassets/newsroom/fact-tank/sales-data/2021/q4/2012-2021-annuity-sales-updated.pdf>.

Other fee structure designs have also been explored by different authors. The idea behind those designs is usually to reduce the insurer's exposure to various risks, such as market volatility and policyholder behaviour. [9] introduce a state-dependent fee structure, where the fee is only paid when the VA account value is below a certain level, and present an analytical formula for a the value of a contract with GMMB rider (without early surrender) under this type of fee structure. [61] study how the fee structure and surrender charges affect the surrender region; they also design surrender charges that eliminate surrender incentives for a financially rational policyholder. Other fee designs have been explored in the literature: [29] considers a general state-dependent fee structure in a Lévy process driven market, whereas [12] study lapse-and-reentry in variable annuities with time-dependent fee structure. Finally, in a recent study, [78] propose a stochastic control approach to determine the optimal fee structure.

Recently, fee structures that are tied to the Chicago Board Options Exchange (CBOE) volatility index, the VIX³, have gained attention in the literature, see [13], [21] and [50]. As mentioned in [13], the motivations behind this new fee design comes directly from the industry. In 2010, SunAmerica issued two new variable annuities whose fees were tied to the volatility index⁴. More recently, America General Life Insurance Company proposed a fee structure that is linked to the VIX for its Polaris series of variable annuities, see Polaris Platinum O-Series prospectus dated May 3rd, 2021⁵. By allowing the fees to move with the volatility index, the insurer expects to better match the cost of hedging with the premium collected. It also permits policyholders to profit from lower fees in low volatility, rising market, environments. The CBOE published two white papers, [33] and [34], illustrating how VIX-linked fee designs can be advantageous to both variable annuity insurers and policyholders. [21] approach the question from a theoretical perspective by analyzing variable annuities without surrender with a fee structure that is tied to the VIX under a Heston-type stochastic volatility model. They provide a closed-form expression for the GMMB rider and observe that such a structure might help realign fee incomes with the value of the financial guarantee. [50] extend the works of [21] by applying the VIX fee designs to a GMWB rider and by adding jumps to the underlying index value process. [13] study fees that are tied to the volatility index by using a Gaussian copula.

In this work, we allow fee structures to be as general as possible, i.e. the fee structure may depend on the time, the fund value, and also on the latent variance process, making it possible to link the fee to the VIX. In the constant fee case, it is well-known that the misalignment between the fees and the value of the financial guarantee creates an incentive for the risk-neutral, rational policyholder to surrender her policy early (see [65]). Since VIX-linked fee structures allow for better alignment of the guaranteed value with the corresponding hedging cost, we expect that such fee designs can also help reduce the insurers' exposure to surrender risk. For this reason, we numerically study the impact of three different VIX-linked fee designs on the optimal surrender strategy. To do so, we use a two-layer continuous-time Markov chain (CTMC) approximation for the fund dynamics inspired by [24]. Two-layer CTMC approximations have recently been used to price derivatives in stochastic volatility models, see [24], [25] and [58], among others. The methodology proposed by [24] for approximating two-dimensional diffusions is not only theoretically appealing and applies to most stochastic volatility models, but also is simple to implement for pricing European and American options. Their approach is especially efficient for a short/medium time horizon. However, for derivatives with very long maturities, such as those involved in variable annuities pricing, the methodology proposed by [24] stretches the computing resource to unacceptable levels. In this paper, we adapt their method to long-maturity cases.

³See https://www.cboe.com/tradable_products/vix/

⁴See Retirement Income Journal available at <https://retirementincomejournal.com/article/sunamerica-links-va-rider-fees-to-volatility-index/>.

⁵See footnote 6 on p.9 of the prospectus (the long-form) available at <https://aig.onlineprospectus.net/AIG/867018103A/index.php?open=POLARIS!5fPLATINUM!5f0-SERIES!5fISP.pdf>.

The main contributions of this paper are as follows:

- We extend the work of [24], done in the context of options pricing, by providing novel efficient algorithms to value options with very long maturities, such as variable annuities, under general stochastic volatility models.
- We propose a methodology to approximate the optimal surrender surface for a VA contract with GMMB rider when the underlying index follows a two-dimensional diffusion process.
- We derive a closed-form analytical expression for the VIX index when the variance process follows a continuous-time Markov chain. The latter may also be used to price VIX derivatives.
- We analyze the optimal surrender strategy for a VA contract with GMMB rider under the assumption that the guarantee fees are linked to the VIX index. In the literature, such an analysis of surrender incentives is usually performed using a constant fee structure, or in a Black-Scholes framework when the fees are state-dependent.

The remainder of the paper is organized as follows. In Section 2, we introduce the market model, the VA contract, and the optimal stopping problem involved in the pricing of variable annuities with surrender. A brief introduction to CTMC approximations for a two-dimensional diffusion process is provided in Section 3. In Section 4, we apply CTMC approximations to VA contract pricing and provide new efficient algorithms. Section 5 provides the numerical results and discusses how VIX-linked fees affect surrender incentives. Section 6 concludes the paper.

2. FINANCIAL SETTING

2.1. Market Model. We consider a filtered probability space $(\Omega, \mathcal{F}, \mathbb{F}, \mathbb{Q})$, where \mathbb{F} is a complete and right-continuous filtration and where \mathbb{Q} denotes the pricing measure for our market, see Remark 2.1. We consider a risky asset, whose price can be described by the two-dimensional process $(S, V) = \{(S_t, V_t)\}_{t \geq 0}$ satisfying

$$(2.1) \quad \begin{aligned} dS_t &= rS_t dt + \sigma_S(V_t)S_t dW_t^{(1)}, \\ dV_t &= \mu_V(V_t) dt + \sigma_V(V_t) dW_t^{(2)}, \end{aligned}$$

with $S_0 = s_0 \in \mathbb{R}_+$ and $V_0 = v_0 \in \mathcal{S}_V$ where \mathcal{S}_V denotes the state-space of V , with $r > 0$ denoting the risk-free rate and with $W = \{(W_t^{(1)}, W_t^{(2)})\}_{t \geq 0}$ is a two-dimensional correlated Brownian motion with cross-variation $[W^{(1)}, W^{(2)}]_t = \rho t$, where $\rho \in [-1, 1]$. For simplicity, V will be referred to as the variance process. We assume that $\mu_V : \mathcal{S}_V \mapsto \mathbb{R}$ is continuous and that $\sigma_S, \sigma_V : \mathcal{S}_V \mapsto \mathbb{R}_+$ are continuously differentiable functions with $\sigma_S(\cdot) > 0$, $\sigma_V(\cdot) > 0$ on the state-space \mathcal{S}_V of V . Further, we suppose that μ_V, σ_V and σ_S are defined such that (2.1) has a unique-in-law weak solution.

Remark 2.1. *In (2.1), we start directly with the dynamics under the risk-neutral measure, hence the form of the market price of volatility risk is not necessary in our setting. However, as pointed out by [74], [45] and [20], a risk-neutral measure may not always exist under stochastic volatility models; additional conditions must be added to the model parameters in order for $\{e^{-rt}S_t\}_{t \geq 0}$ to be a true martingale. A list of common SV models are reported in Table 1 below, along with conditions for the martingale property to hold under the risk-neutral measure.*

2.2. Variable Annuity Contract. A policyholder enters a variable annuity contract by depositing an initial premium F_0 into a sub-account, which is then invested in a fund tracking the financial market. For simplicity, we will assume that the sub-account is invested in the risky asset S . The policyholder often has the right to surrender the contract, or lapse, prior to maturity. This additional flexibility is often called surrender option (or surrender right) in the literature and significantly complicates the valuation of variable annuity contracts. Below we discuss the

⁶The condition stated in [20], Proposition 2.5.4 is automatically satisfied by requiring the correlation parameter ρ to be non-positive, as pointed out by [31].

⁷If $b \neq 0$, then we must also impose $\kappa\theta \geq \sigma^2/2$ for the model to be well-defined.

Model Name	Dynamics	Parameters	Cond. for Martingale Measure
Heston (1993) [40]	$dS_t = rS_t dt + \sqrt{V_t}S_t dW_t^{(1)}$ $dV_t = \kappa(\theta - V_t) dt + \sigma\sqrt{V_t} dW_t^{(2)}$	$S_0 > 0,$ $\kappa, \theta, \sigma, V_0 > 0$	No additional cond. [20], Proposition 2.5.1
3/2 (1997) [41]	$dS_t = rS_t dt + S_t/\sqrt{V_t} dW_t^{(1)}$ $dV_t = \kappa(\theta - V_t) dt - \sigma\sqrt{V_t} dW_t^{(2)}$	$S_0 > 0,$ $\kappa, \theta, \sigma, V_0 > 0$ with $\kappa\theta \geq \sigma^2/2$	$\rho \leq 0,$ [20], Proposition 2.5.4 ⁶
4/2 (2017) [36]	$dS_t = rS_t dt + S_t [a\sqrt{V_t} + b/\sqrt{V_t}] dW_t^{(1)}$ $dV_t = \kappa(\theta - V_t) dt + \sigma\sqrt{V_t} dW_t^{(2)}$	$a, b \in \mathbb{R}, S_0 > 0,$ $\kappa, \theta, \sigma, V_0 > 0,$ with $\kappa\theta \geq \sigma^2/2$ ⁷	$\sigma^2 \leq 2\kappa\theta + \min(0, 2\rho\sigma b)$ [36], Section 2.2
Hull-White (1987) [43]	$dS_t = rS_t dt + \sqrt{V_t}S_t dW_t^{(1)}$ $dV_t = \alpha V_t dt + \beta V_t dW_t^{(2)}$	$S_0 > 0,$ $\alpha, \beta, V_0 > 0$	$\rho \leq 0,$ [45], Theorem 1 or [20], Proposition 2.5.10
Scott (1987) [71], p.426	$dS_t = rS_t dt + e^{V_t}S_t dW_t^{(1)}$ $dV_t = \kappa(\theta - V_t) dt + \sigma dW_t^{(2)}$	$S_0 > 0,$ $\kappa, \theta, V_0 \in \mathbb{R}, \sigma > 0$	$\rho \leq 0,$ [45], Theorem 1
α -Hypergeometric (2016) [27]	$dS_t = rS_t + e^{V_t}S_t dW_t^{(1)}$ $dV_t = (a - be^{\alpha V_t}) dt + \sigma dW_t^{(2)}$	$S_0 > 0,$ $\alpha, b, \sigma > 0, a, V_0 \in \mathbb{R}$	If $\alpha \geq 2$ or $\alpha < 2$ and either $\rho \leq 0, \alpha > 1$ or $\alpha = 1$ and $b \geq \rho\sigma$ [27], Proposition 6

TABLE 1. Examples of stochastic volatility models

risk-neutral valuation approach for a variable annuity, under both the assumption that the policyholder makes use of her surrender right or does not.

To do so, we consider a finite time horizon $T \in \mathbb{R}_+$ and let $F = \{F_t\}_{0 \leq t \leq T}$ denote the variable annuity fund (or sub-account) process. Moreover, we let $C : [0, T] \times \mathbb{R}_+ \times \mathcal{S}_V \rightarrow \mathbb{R}_+$ denote the fee function and let the continuously compounded fee rate process $\{c_t\}_{0 \leq t \leq T}$ be defined as

$$(2.2) \quad c_t := C(t, F_t, V_t), \quad 0 \leq t \leq T,$$

where C is assumed to be continuous or bounded and such that (2.4) has a unique-in-law weak solution. We allow the fee structure to be as general as possible. This setting includes, among others, state-dependent fee structures (see [9], [29], [61]), VIX-linked fee structures (see [21], [50], [13]), and time-dependent fee structures (see [12]).

We assume that the fees are paid continuously out of the fund at a rate c_t , so that the fund value is given by

$$(2.3) \quad F_t = S_t e^{-\int_0^t c_u du}, \quad 0 \leq t \leq T,$$

with $F_0 = S_0$. Using Itô's lemma, the dynamics of F under the risk-neutral measure are

$$(2.4) \quad \begin{aligned} dF_t &= (r - c_t)F_t dt + \sigma_S(V_t)F_t dW_t^{(1)}, \\ dV_t &= \mu_V(V_t) dt + \sigma_V(V_t) dW_t^{(2)}. \end{aligned}$$

Throughout this paper, $\mathbb{E}_{t,x,y}[\cdot]$ is short-hand notation for $\mathbb{E}[\cdot | F_t = x, V_t = y]$ and $\mathbb{E}_t[\cdot]$ for $\mathbb{E}[\cdot | \mathcal{F}_t]$, with $x \in \mathbb{R}_+, y \in \mathcal{S}_V$ and $t \in [0, T]$. We also use $\mathbb{E}_{x,y}[\cdot]$ to denote $\mathbb{E}_{0,x,y}[\cdot]$.

We focus on a variable annuity with a guaranteed minimum maturity benefit (GMMB) whose payoff at maturity T is $\max(G, F_T)$, where $G \in \mathbb{R}_+$ is a predetermined guaranteed amount. Given $(F_t, V_t) = (x, y)$, the time- t risk-neutral value of the variable annuity assuming that it will not be surrendered early is

$$(2.5) \quad v_e(t, x, y) := \mathbb{E}_{t,x,y} \left[e^{-r(T-t)} \max(G, F_T) \right].$$

On early surrender, the policyholder receives the value of the VA sub-account, reduced by a penalty which, in our setting, can depend on time and on the value of the variance process V . When no surrender occurs, the maturity benefit is paid at T .

More formally, the VA reward (or gain) function $\varphi : [0, T] \times \mathbb{R}_+ \times \mathcal{S}_V \rightarrow \mathbb{R}_+$ is defined by

$$(2.6) \quad \varphi(t, x, y) = \begin{cases} g(t, y)x & \text{if } t < T, \\ \max(G, x) & \text{if } t = T, \end{cases}$$

where $g : [0, T] \times \mathcal{S}_V \rightarrow [0, 1]$ is continuous, non-decreasing in time and satisfies $\lim_{t \rightarrow T^-} g(t, y) = 1 \forall y \in \mathcal{S}_V$. In practice, we usually consider the surrender charge (as a percentage of the account value), $1 - g(\cdot, \cdot)$. A common form for the surrender charge function in the literature is $g(t, y) = e^{-k(T-t)}$ for some constant $k \geq 0$, see for example [61], [72], [5] and [46]. It is the first time, to the best of our knowledge, that variance-dependent surrender charges are considered.

Remark 2.2. For $x < G$, the function $t \mapsto \varphi(t, x, y)$ is discontinuous at T since

$$\lim_{t \rightarrow T^-} \varphi(t, x, y) = g(t, y)x \leq x < G = \varphi(T, x, y).$$

Under the assumption that the policyholder maximizes the risk-neutral value of her VA contract, the time- t value of the variable annuity policy is given by

$$(2.7) \quad v(t, x, y) = \sup_{\tau \in \mathcal{T}_{t, T}} \mathbb{E}_{t, x, y}[e^{-r(\tau-t)} \varphi(\tau, F_\tau, V_\tau)],$$

where $\mathcal{T}_{t, T}$ is the (admissible) set of all stopping times taking values in the interval $[t, T]$.

When the fee function is time-independent, the fund process is time-homogeneous, and (2.7) is equivalent to

$$(2.8) \quad v(t, x, y) = \sup_{\tau \in \mathcal{T}_0, T-t} \mathbb{E}_{x, y}[e^{-r\tau} \varphi(\tau + t, F_\tau, V_\tau)].$$

Similarly to the early exercise premium in the American option literature, the value of the right to surrender, denoted by $e : [0, T] \times \mathbb{R}_+ \times \mathcal{S}_V \rightarrow \mathbb{R}_+$, is defined by

$$e(t, x, y) := v(t, x, y) - v_e(t, x, y).$$

3. CONTINUOUS-TIME MARKOV CHAIN APPROXIMATION

The CTMC framework outlined in this section has been proposed by [24] for exotic option pricing under stochastic local volatility models. The general idea is to approximate the two-dimensional stock price process by a two dimensional continuous-time Markov chain. This is done by first approximating the variance process by a CTMC, and then by replacing the variance process by its CTMC approximation in the underlying price process. The resulting regime-switching diffusion process is then further approximated by a CTMC, yielding a two-dimensional CTMC process which converges weakly to the original two-dimensional diffusion process, providing that the generator of the CTMC is chosen correctly.

First, we shall briefly recall the basics of continuous-time Markov chains, following sections 6.9 and 6.10 of [37]. The stochastic process $\tilde{X} = \{\tilde{X}_t\}_{t \geq 0}$ taking values on some discrete state-space $\mathcal{S}_{\tilde{X}}$ is called a continuous-time Markov chain if it satisfies the following property (a.k.a. *Markov property*):

$$\mathbb{P}(\tilde{X}_{t_n} = \tilde{x}_j | \tilde{X}_{t_1} = \tilde{x}_{i_1}, \dots, \tilde{X}_{t_{n-1}} = \tilde{x}_{i_{n-1}}) = \mathbb{P}(\tilde{X}_{t_n} = \tilde{x}_j | \tilde{X}_{t_{n-1}} = \tilde{x}_{i_{n-1}})$$

for all $\tilde{x}_j, \tilde{x}_{i_1}, \dots, \tilde{x}_{i_{n-1}} \in \mathcal{S}_{\tilde{X}}$ and any time sequence $t_1 < t_2 < \dots < t_n$.

The *transition probability* $p_{ij}(s, t)$, from state $\tilde{x}_i \in \mathcal{S}_{\tilde{X}}$ at time s to state $\tilde{x}_j \in \mathcal{S}_{\tilde{X}}$ at time t , is defined by

$$p_{ij}(s, t) = \mathbb{P}(\tilde{X}_t = \tilde{x}_j | \tilde{X}_s = \tilde{x}_i), \quad s \leq t.$$

The chain is said to be *homogeneous* if $p_{ij}(s, t) = p_{ij}(0, t - s)$ for any $i, j, s \leq t$. In that case, we use $p_{ij}(t - s)$ to denote $p_{ij}(s, t)$.

Now assume that \tilde{X} is time-homogeneous and $\mathcal{S}_{\tilde{X}}$ is finite.

The family $\{\mathbf{P}_t := [p_{ij}(t)]_{|\mathcal{S}_{\tilde{X}}| \times |\mathcal{S}_{\tilde{X}}|}\}_{t \geq 0}$ of *transition probability matrices* is referred as the *transition semigroup* of the Markov chain.

For an infinitesimal period of length $h > 0$, it can be shown that there exist constants $\{q_{ij}\}$, also called *transition rates*, such that

$$(3.1) \quad p_{ij}(h) = \begin{cases} q_{ij}h + c(h) & \text{if } i \neq j \\ 1 + q_{ij}h + c(h) & \text{if } i = j, \end{cases}$$

for $1 \leq i, j \leq |\mathcal{S}_{\tilde{X}}|$, where c is a function satisfying $\lim_{h \rightarrow 0} \frac{c(h)}{h} = 0$.

From the above, we can conclude that the transition rates must satisfy

$$(3.2) \quad q_{ij} \geq 0, \text{ if } i \neq j \quad \text{and} \quad q_{ij} \leq 0, \text{ if } i = j,$$

and

$$(3.3) \quad \sum_{j=1}^m q_{ij} = 0, \quad i = 1, 2, \dots, m.$$

The matrix $\mathbf{Q} := [q_{ij}]_{|\mathcal{S}_{\tilde{X}}| \times |\mathcal{S}_{\tilde{X}}|}$ is called the *generator* of \tilde{X} . Under some technical conditions⁸, it can be shown that the transition probability matrix \mathbf{P}_t has the following matrix exponential representation:

$$(3.4) \quad \mathbf{P}_t = \exp(\mathbf{Q}t) = \sum_{k=0}^{\infty} \frac{(\mathbf{Q}t)^k}{k!}.$$

Assumption 3.1. *The fee function defined in (2.2) is time-independent and denoted by c . That is, $C(t, x, y) = c(x, y)$ for all $0 \leq t \leq T$. Moreover, we only consider functions c that are continuous or bounded.*

Henceforth, we consider that Assumption 3.1 holds. That is, we assume that the fee function is time-independent so that the fund process is time-homogeneous. For the CTMC approximation of diffusion processes with time-dependent coefficients, see [30].

3.1. Approximation of the Variance Process $\{V_t\}_{t \geq 0}$. We construct a CTMC $\{V_t^{(m)}\}_{t \geq 0}$ taking values on a finite state-space $\mathcal{S}_V^{(m)} := \{v_1, v_2, \dots, v_m\}$, with $v_i \in \mathcal{S}_V$ and $m \in \mathbb{N}$, that converges weakly to $\{V_t\}_{t \geq 0}$ as $m \rightarrow \infty$. Weak convergence of $V^{(m)}$ to V , is denoted by $V^{(m)} \Rightarrow V$. Several approaches are available in the literature to construct the finite state-space $\mathcal{S}_V^{(m)}$, from simple uniform to non-uniform grids (see [76] [64], [57] for examples of non-uniform grids). Most grid constructions require the specification of the two boundary states $v_1, v_m \in \mathcal{S}_V$. The lower (resp. upper) boundary v_1 (resp. v_m) must be sufficiently small (resp. large) to ensure that the grid covers a reasonably large portion of the state-space of the original process. This can be done naively by setting $v_1 = \alpha V_0$ and $v_m = \beta V_0$ for a small (resp. large) constant α (resp. β), or by using the first two moments of the variance process to select the boundary values (see [48],[22], [23] and [56] for details.) The specific grid selected for the numerical analysis performed in this paper is discussed in more details in Section 5.

Once the state-space is chosen, the approximating CTMC $\{V_t^{(m)}\}_{t \geq 0}$ is defined via its generator $\mathbf{Q}^{(m)} = [q_{ij}^{(m)}]_{m \times m}$. This generator is constructed so that the first two moments of the transition density of the variance process $\{V_t\}_{t \geq 0}$ and the approximating CTMC $\{V_t^{(m)}\}_{t \geq 0}$ coincide; these are the so-called *local consistency conditions*, see [52] and [57]. More precisely, the elements q_{ij} ,

⁸More precisely, the semigroup $\{P_t\}$ must be standard—that is, $p_{ii}(t) \rightarrow 1$ and $p_{ij}(t) \rightarrow 0$ as $t \downarrow 0$ —and uniform— $\sup_i -q_{ii} < \infty$, see [37], Definition 6.9.4, Theorem 6.10.1 and 6.10.6 for details.

$1 \leq i, j \leq m$ of the generator of $V^{(m)}$ are chosen so that for a small time increment $h \ll T$,

$$(3.5) \quad \begin{aligned} \mathbb{E}_t \left[V_{t+h}^{(m)} - V_t^{(m)} \right] &= \mathbb{E}_t [V_{t+h} - V_t] \simeq \mu_V(V_t)h, \quad \text{and} \\ \mathbb{E}_t \left[\left(V_{t+h}^{(m)} - V_t^{(m)} \right)^2 \right] &= \mathbb{E}_t \left[(V_{t+h} - V_t)^2 \right] \simeq \sigma_V^2(V_t)h, \end{aligned}$$

for all $t \geq 0$. To ensure that the local consistency conditions are satisfied, we use the generator proposed by [57] and given by⁹

$$(3.6) \quad q_{ij} = \begin{cases} \frac{\sigma_V^2(v_i) - \delta_i \mu_V(v_i)}{\delta_{i-1}(\delta_{i-1} + \delta_i)} & j = i - 1 \\ -q_{i,i-1} - q_{i,i+1} & j = i \\ \frac{\sigma_V^2(v_i) + \delta_{i-1} \mu_V(v_i)}{\delta_i(\delta_{i-1} + \delta_i)} & j = i + 1 \\ 0 & j \neq i, i - 1, i + 1, \end{cases}$$

for $2 \leq i \leq m - 1$ and $1 \leq j \leq m$ and where $\delta_i = v_{i+1} - v_i$, $i = 1, 2, \dots, m - 1$. On the borders, we set $q_{12} = \frac{|\mu_V(v_1)|}{\delta_1}$, $q_{11} = -q_{12}$, $q_{m,m-1} = \frac{|\mu_V(v_m)|}{\delta_{m-1}}$, $q_{m,m} = -q_{m,m-1}$; and 0 elsewhere.

To obtain a well-defined $\mathbf{Q}^{(m)}$ matrix, the transition rates in (3.6) must also satisfy the conditions in (3.2). Hence, for $2 \leq i \leq m - 1$,

- if $\mu_V(v_i) < 0$, then we must have

$$(3.7) \quad \delta_{i-1} \leq \frac{\sigma_V^2(v_i)}{|\mu_V(v_i)|},$$

in order for $q_{i,i+1}$ to be well defined (that is, $q_{i,i+1} \geq 0$), and

- if $\mu_V(v_i) > 0$, then we must have

$$(3.8) \quad \delta_i \leq \frac{\sigma_V^2(v_i)}{\mu_V(v_i)},$$

in order for $q_{i,i-1} \geq 0$.

- when $\mu_V(v_i) = 0$ then no additional condition needs to be added.

Remark 3.2. A sufficient condition for (3.7) and (3.8) to hold is

$$(3.9) \quad \max_{1 \leq i \leq m-1} \delta_i \leq \min_{1 \leq i \leq m-1} \frac{\sigma_V^2(v_i)}{|\mu_V(v_i)|}.$$

When this condition is not satisfied, more points should be added to the existing grid. However, it can sometimes be too restrictive, particularly in the case of approximating a two-dimensional process, where adding more points to the state-space becomes too expensive computationally. In that case, condition (3.9) may be replaced by a simple verification of (3.7) and (3.8) which is less restrictive. However, from a numerical perspective, we observe that such conditions are not necessary to obtain good approximation results.

The transition rates on the boundaries of the state-space are set so that the absolute instantaneous means are maintained at the endpoints. Other schemes could have also been employed (see [19],[64]), but we observed that all of these schemes are equivalent numerically.

3.2. Approximation of the Fund Value Process $\{F_t\}_{0 \leq t \leq T}$. The CTMC approximating $\{F_t\}_{t \geq 0}$ is constructed by first replacing the variance process appearing in the drift and diffusion coefficients by their CTMC approximations, and then by further approximating the resulting regime-switching diffusion process by another CTMC. The resulting two-dimensional regime-switching CTMC can then be mapped to a one-dimensional CTMC on an enlarged state-space. Lemma 3.3 below allows for the removal of the correlation between the Brownian motions in (2.4), which is necessary to construct the CTMC approximation of $\{F_t\}_{t \geq 0}$.

⁹An advised reader will notice some difference between the transition rates stated above, and the ones that appear in [57]. However, one can show that the two rate matrices are equivalent with some simple algebra.

Lemma 3.3 (Lemma 1 of [24]). *Let F and V be defined as in (2.4). Define $\gamma(x) := \int^x \frac{\sigma_S(u)}{\sigma_V(u)} du$ and $X_t := \ln(F_t) - \rho\gamma(V_t)$, $t \in [0, T]$. Then X satisfies*

$$(3.10) \quad \begin{aligned} dX_t &= \mu_X(X_t, V_t) dt + \sigma_X(V_t) dW_t^* \\ dV_t &= \mu_V(V_t) dt + \sigma_V(V_t) dW_t^{(2)}, \end{aligned}$$

where W_t^* is a standard Brownian motion $W_t^* := \frac{W_t^{(1)} - \rho W_t^{(2)}}{\sqrt{1-\rho^2}}$ independent of $W_t^{(2)}$, $\sigma_X(y) := \sqrt{1-\rho^2}\sigma_S(y)$ and $\mu_X(x, y) := r - c(e^{x+\rho\gamma(y)}, y) - \frac{\sigma_S^2(y)}{2} - \rho\psi(y)$, and

$$\begin{aligned} \psi(y) &:= \mathcal{L}_v\gamma(y) = \mu_V(y)\gamma'(y) + \frac{1}{2}\sigma_V^2(y)\gamma''(y) \\ &= \mu_V(y)\frac{\sigma_S(y)}{\sigma_V(y)} + \frac{1}{2}[\sigma_V(y)\sigma_S'(y) - \sigma_V'(y)\sigma_S(y)], \end{aligned}$$

for $x \in \mathbb{R}, y \in \mathcal{S}_V$.

The proof relies on the multidimensional Itô formula (see Lemma 1 of [24] for details). Given the CTMC approximation of the process $V^{(m)}$ and its generator $\mathbf{Q}^{(m)}$, the diffusion process in (3.10) can now be approximated by a regime-switching diffusion process $\{X_t^{(m)}\}_{t \geq 0}$:

$$(3.11) \quad dX_t^{(m)} = \mu_X(X_t^{(m)}, V_t^{(m)}) dt + \sigma_X(V_t^{(m)}) dW_t^*,$$

where regimes are determined by the states of the approximated variance process, $\{v_1, v_2, \dots, v_m\}$. To construct a regime-switching CTMC $(X_t^{(m,N)}, V_t^{(m)})$ approximating the regime-switching diffusion $(X_t^{(m)}, V_t^{(m)})$, we fix a state for the variance process $V_t^{(m)}$ (or equivalently a regime) and construct a CTMC approximation for $X_t^{(m)}$ given that $V_t^{(m)}$ is in that state. This is done using the procedure described in Section 3.1 for a one-dimensional diffusion process. The procedure is then repeated for each state in $\mathcal{S}_V^{(m)}$, and the approximating CTMCs are combined with $V^{(m)}$ to obtain the final regime-switching CTMC.

More precisely, let $X_t^{(m,N)}$ be the CTMC approximation of $X_t^{(m)}$ taking values on a finite state-space $\mathcal{S}_X^{(N)} = \{x_1, x_2, \dots, x_N\}$, $N \in \mathbb{N}$. For each $v_l \in \mathcal{S}_V^{(m)}$, we define the generator $\mathbf{G}_l^{(N)} = [\lambda_{ij}^l]_{N \times N}$ of $X_t^{(m,N)}$ given that the variance process is in state v_l at time $t \geq 0$ by

$$(3.12) \quad \lambda_{ij}^l = \begin{cases} \frac{\sigma_X^2(v_l) - \delta_i^x \mu_X(x_i, v_l)}{\delta_{i-1}^x (\delta_{i-1}^x + \delta_i^x)} & j = i-1 \\ -\lambda_{i,i-1}^l - \lambda_{i,i+1}^l & j = i \\ \frac{\sigma_X^2(v_l) + \delta_{i-1}^x \mu_X(x_i, v_l)}{\delta_i^x (\delta_{i-1}^x + \delta_i^x)} & j = i+1 \\ 0 & j \neq i, i-1, i+1, \end{cases}$$

for $2 \leq i \leq N-1$ and $1 \leq j \leq N$, where $\delta_i^x = x_{i+1} - x_i$, $i = 1, 2, \dots, N-1$. On the boundaries, we set $\lambda_{12}^l = \frac{|\mu_X(x_1, v_l)|}{\delta_1^x}$, $\lambda_{11}^l = -\lambda_{12}^l$, $\lambda_{N,N-1}^l = \frac{|\mu_X(x_N, v_l)|}{\delta_{N-1}^x}$, $\lambda_{N,N}^l = -\lambda_{N,N-1}^l$, and 0 elsewhere.

Using $V^{(m)}$ and the relation presented in Lemma 3.3, the approximated fund process $F^{(m,N)}$, which approximates F , is defined by

$$(3.13) \quad F_t^{(m,N)} := \exp \left\{ X_t^{(m,N)} + \rho\gamma(V_t^{(m)}) \right\}, \quad 0 \leq t \leq T.$$

Remark 3.4 (Convergence of the approximation). *Such a construction of the regime-switching CTMC ensures that the two-dimensional process $(X_t^{(m,N)}, V_t^{(m)})$ converges weakly to (X_t, V_t) as $m, N \rightarrow \infty$. The main idea is to show that the generator of $(X_t^{(m,N)}, V_t^{(m)})$ is uniformly close to the infinitesimal generator of (X_t, V_t) as $m, N \rightarrow \infty$, to then conclude that $(X_t^{(m,N)}, V_t^{(m)}) \Rightarrow (X_t, V_t)$ using the results of [32] which relies on semi-group theory. Moreover, since the function $h: \mathbb{R} \times \mathcal{S}_V \rightarrow \mathbb{R}_+$ defined by $h(x, y) = e^{x+\rho\gamma(y)}$ is continuous, we have that $F^{(m,N)} \Rightarrow F$ by the continuous mapping Theorem, see [14] Theorem 2.7. For one-dimensional processes, intuition and*

detailed explanations of the proof can be found in [64], Section 5 (or in the unabridged version of the paper [63], Section 6); for stochastic volatility models, see [24], Section 2.4.

The last step is to convert the regime-switching CTMC $(X_t^{(m,N)}, V_t^{(m)})$ into a one-dimensional CTMC process $Y_t^{(m,N)}$ on an enlarged state-space $\mathcal{S}_Y^{(m,N)} := \{1, 2, \dots, mN\}$. This is done in Theorem 1 of [15], reproduced below.

Proposition 3.5 (Theorem 1 of [15]). *Consider a regime-switching CTMC $(X^{(m,N)}, V^{(m)})$ taking values in $\mathcal{S}_X^{(N)} \times \mathcal{S}_V^{(m)}$ where $\mathcal{S}_X^{(N)} = \{x_1, x_2, \dots, x_N\}$ and $\mathcal{S}_V^{(m)} = \{v_1, v_2, \dots, v_m\}$; and another one-dimensional CTMC, $\{Y_t^{(m,N)}\}_{0 \leq t \leq T}$, taking values in $\mathcal{S}_Y^{(m,N)} := \{1, 2, \dots, mN\}$ and its transition rate matrix $\mathbf{G}^{(m,N)}$ given by*

$$(3.14) \quad \begin{pmatrix} q_{11}\mathbf{I}_N + \mathbf{G}_1^{(N)} & q_{12}\mathbf{I}_N & \cdots & q_{1m}\mathbf{I}_N \\ q_{21}\mathbf{I}_N & q_{22}\mathbf{I}_N + \mathbf{G}_2^{(N)} & \cdots & q_{2m}\mathbf{I}_N \\ \vdots & \vdots & \ddots & \vdots \\ q_{m1}\mathbf{I}_N & q_{m2}\mathbf{I}_N & \cdots & q_{mm}\mathbf{I}_N + \mathbf{G}_m^{(N)} \end{pmatrix},$$

where \mathbf{I}_N is the $N \times N$ identity matrix, $\mathbf{G}_l^{(N)} = [\lambda_{ij}^l]_{N \times N}$, $l = 1, 2, \dots, m$ and $\mathbf{Q}^{(m)} = [q_{ij}]_{m \times m}$ are the generators defined in (3.12) and (3.6), respectively. Define the function $\psi : \mathcal{S}_X^{(N)} \times \mathcal{S}_V^{(m)} \rightarrow \mathcal{S}_Y^{(m,N)}$ by $\psi(x_n, v_l) = (l-1)N + n$ and its inverse $\psi^{-1} : \mathcal{S}_Y^{(m,N)} \mapsto \mathcal{S}_X^{(N)} \times \mathcal{S}_V^{(m)}$ by $\psi^{-1}(n_y) = (x_n, v_l)$ for $n_y \in \mathcal{S}_Y^{(m,N)}$, where $n \leq N$ is the unique integer such that $n_y = (l-1)N + n$ for some $l \in \{1, 2, \dots, m\}$. Then, we have

$$\mathbb{E} \left[\Psi(X^{(m,N)}, V^{(m)}) | X_0^{(m,N)} = x_i, V_0^{(m)} = v_k \right] = \mathbb{E} \left[\Psi(\psi^{-1}(Y^{(m,N)})) | Y_0 = (k-1)N + i \right],$$

for any path-dependent function Ψ such that the expectation on the left-hand side is finite.

4. VARIABLE ANNUITY PRICING VIA CTMC APPROXIMATION

In this section, we use the CTMC approximation of the fund value process to price variable annuities under different surrender strategies. We provide a simple way to approximate the optimal surrender surface, which is the extension in three dimensions of the exercise boundary for two-dimensional processes. The present section is based on [24] and [25], in which CTMC approximation are used for option pricing.

Recall that $(X^{(m,N)}, V^{(m)})$ is the regime-switching CTMC approximation of (X, V) (see Lemma 3.3) taking values in a finite state-space $\mathcal{S}_X^{(N)} \times \mathcal{S}_V^{(m)}$ where $\mathcal{S}_X^{(N)} = \{x_1, x_2, \dots, x_N\}$, $N \in \mathbb{N}$; and $\mathcal{S}_V^{(m)} = \{v_1, v_2, \dots, v_m\}$, $m \in \mathbb{N}$. We have also defined $F^{(m,N)}$ in terms of $(X^{(m,N)}, V^{(m)})$ in (3.13).

Throughout this section, we denote by $\{\mathbf{e}_{ik}\}_{i,k=1}^{N,m}$ the standard basis in \mathbb{R}^{mN} , i.e. \mathbf{e}_{ik} represents a row vector of size $1 \times mN$ having a value of 1 in the $(k-1)N + i$ -th entry and 0 elsewhere.

4.1. Variable Annuity without Early Surrenders. Consider an initial premium $F_0 > 0$ and let $V_0 \in \mathcal{S}_V$. The risk-neutral value of a variable annuity contract assuming no early surrenders can be approximated by

$$(4.1) \quad \begin{aligned} v_e(0, F_0, V_0) &= \mathbb{E} \left[e^{-rT} \max(G, F_T) | F_0, V_0 \right] \\ &\approx \mathbb{E} \left[e^{-rT} \max(G, F_T^{(m,N)}) | X_0^{(m,N)} = x_i, V_0^{(m)} = v_k \right]. \end{aligned}$$

Here, we assume¹⁰ that $x_i \in \mathcal{S}_X^{(N)}$ and $v_k \in \mathcal{S}_V^{(m)}$, with $x_i = \ln(F_0) - \rho\gamma(V_0)$.

¹⁰If $X_0^{(m,N)}$ and $V_0^{(m)}$ are not part of their respective grids, then the two points can be added to the grids, or the option price must be linearly interpolated between grid points, see Remark 5.1 for details.

Proposition 4.1. *Let $F_0 > 0$ be the initial premium, with $X_0^{(m,N)} = \ln(F_0) - \rho\gamma(V_0) = x_i \in \mathcal{S}_X^{(N)}$ and $V_0 = v_k \in \mathcal{S}_V$. The risk-neutral value at time 0 of a variable annuity contract held until maturity T and with guaranteed amount $G > 0$ can be approximated by*

$$(4.2) \quad \begin{aligned} v_e^{(m,N)}(0, F_0, V_0) &:= \mathbb{E}[e^{-rT} \max(G, F_T^{(m,N)}) | F_0^{(m,N)} = F_0, V_0^{(m)} = V_0] \\ &= e^{-rT} \mathbf{e}_{ik} \exp\{T\mathbf{G}^{(m,N)}\} \mathbf{H}, \end{aligned}$$

where $\mathbf{G}^{(m,N)}$ is defined in (3.14) and \mathbf{H} is a column vector of size $mN \times 1$ whose $(l-1)N + n$ -th entry is given by

$$(4.3) \quad h_{(l-1)N+n} = \max\left(G, e^{x_n + \rho\gamma(v_l)}\right), \quad 1 \leq l \leq m, 1 \leq n \leq N.$$

The proof is straightforward by noticing that (4.2) is the matrix representation of the conditional expectation of a (function of a) discrete one-dimensional random variable whose conditional probability mass function is given by the transitional probabilities $p_{(k-1)N+i,j}(T)$, $1 \leq j \leq mN$, with $\mathbf{P}(T) = [p_{ij}(T)]_{mN \times mN} = \exp\{T\mathbf{G}^{(m,N)}\}$ as per (3.4).

The algorithm to approximate the value of a variable annuity without early surrenders is straightforward from the last proposition.

Remark 4.2 (Convergence of VA prices without early surrenders). *As per Remark 3.4, we know that $F^{(m,N)} \Rightarrow F$, as $m, N \rightarrow \infty$. From the continuous mapping theorem, c.f. Theorem 2.7 of [14], we also know that $\varphi(T, F_T^{(m,N)}, V_T^{(m)}) \Rightarrow \varphi(T, F_T, V_T)$; implying the convergence of the corresponding VA prices $\mathbb{E}[\varphi(T, F_T^{(m,N)}, V_T^{(m)})] \rightarrow \mathbb{E}[\varphi(T, F_T, V_T)]$, Theorem 3.6 of [14]. Convergence analysis of the two-layers CTMC approximation in the context of European option pricing is performed in [59].*

4.1.1. *Fast Algorithm.* When we consider a typical time-horizon of 10, 15 or 20 years as is often the case in VA pricing, the probability for the fund or the volatility processes to reach high (resp. low) value is higher than when shorter maturities are concerned, and so the grid's upper (resp. lower) bound must be set to a higher (resp. lower) value. This complicates the pricing of VAs compared to financial option pricing (generally written for short or medium time-horizon), since we need more discretization points m and N in order to capture the distribution of the variance and the fund value process correctly. Theoretically, this is not a problem; however several numerical issues can be encountered when computing the price. First, the generator matrix $\mathbf{G}^{(m,N)}$ can become very large and thus require a large amount of storage space, which may cause memory problems. Second, calculating the exponential of a large sparse $mN \times mN$ matrix over a long time horizon is time-consuming.

Using the tower property of conditional expectations and an approximation based on the assumption that the variance process remains constant over small time periods, we propose a new algorithm that speeds up the pricing of the VA contract without early surrenders (see Algorithm 1). The main idea behind the new algorithm resides in the use of nested conditional expectations. More precisely, for $h = T/M$, $M \in \mathbb{N}$, we use

$$\mathbb{E}\left[e^{-rT} \varphi\left(T, e^{X_T^{(m,N)} + \rho\gamma(V_T^{(m)})}, V_T^{(m)}\right)\right] = \mathbb{E}[\tilde{\varphi}(kh)], \quad k = 1, 2, \dots, M-2$$

with $\tilde{\varphi}(kh) = \mathbb{E}[\tilde{\varphi}((k+1)h) | \mathcal{F}_{kh}]$ and $\tilde{\varphi}((M-1)h) = \mathbb{E}\left[\varphi\left(T, e^{X_T^{(m,N)} + \rho\gamma(V_T^{(m)})}, V_T^{(m)}\right) | \mathcal{F}_{(M-1)h}\right]$.

The approximation used in Algorithm 1 follows from Proposition 4.3 presented below.

Proposition 4.3. *Let $h > 0$ with $h \ll T$ and $0 \leq t \leq T - h$. For any function ϕ such that the expectation on the left-hand side of (4.4) is finite, we have that*

$$(4.4) \quad \begin{aligned} \mathbb{E}\left[\phi\left(t+h, X_{t+h}^{(m,N)}, V_{t+h}^{(m)}\right) | X_t^{(m,N)} = x_i, V_t^{(m)} = v_k\right] \\ = \sum_{j=1}^m \mathbb{E}\left[\phi\left(t+h, X_{t+h}^{(m,N)}, V_{t+h}^{(m)}\right) | V_t^{(m)} = v_j, X_t^{(m,N)} = x_i\right] \end{aligned}$$

$$\times \mathbb{P} \left(V_{t+h}^{(m)} = v_j | V_t^{(m)} = v_k \right) + c(h),$$

where $c(h)$ is a function satisfying $\lim_{h \rightarrow 0} \frac{c(h)}{h} = 0$.

The proof of Proposition 4.3 is reported in Appendix A.1.

Using the last proposition allows us to work with the matrices $\{\mathbf{G}_j^{(N)}\}_{j=1}^m$ and $\mathbf{Q}^{(m)}$ separately, so that the new algorithm now requires m times the calculation of the exponential of a $N \times N$ matrix and one time the exponential of a $m \times m$ matrix over small time-intervals. Hence, by reducing the size of the matrix in the matrix exponential and the length of the time interval over which the exponential is calculated allows to reduce the computation time significantly and to manage the memory space more effectively. Also, note that the added cost of computing $m + 1$ matrix exponentials (rather than only one) is counterbalanced by the reduced cost of computing the exponential of smaller matrices over a short time interval h .

The following notation is used in Algorithm 1 below.

- (1) We use $M \in \mathbb{N}$ time steps of length $\Delta_M = T/M$.
- (2) $\mathbf{B} = [b_{jn}]_{j,n=1}^{m,N}$ denotes a matrix of size $m \times N$, containing the value of the VA contract. More precisely, the matrix \mathbf{B} is updated at each time step, so that after the first iteration, $b_{jn} \approx \mathbb{E} \left[e^{-rT} \varphi(T, e^{X_T^{(m,N)} + \rho\gamma(V_T^{(m)})}, V_T^{(m)}) | X_{T-\Delta_M}^{(m,N)} = x_n, V_{T-\Delta_M}^{(m)} = v_j \right]$; after the second iteration, $b_{jn} \approx \mathbb{E} \left[e^{-rT} \varphi(T, e^{X_T^{(m,N)} + \rho\gamma(V_T^{(m)})}, V_T^{(m)}) | X_{T-2\Delta_M}^{(m,N)} = x_n, V_{T-2\Delta_M}^{(m)} = v_j \right]$, and so on.
- (3) $\mathbf{B}_{*,n} = [b_{jn}]_{j=1}^m$ denotes the n -th column of \mathbf{B} , $n = 1, 2, \dots, N$,
- (4) $\mathbf{B}_{j,*} = [b_{jn}]_{n=1}^N$ denotes the j -th row of \mathbf{B} , $j = 1, 2, \dots, m$.
- (5) The symbol \top indicates the matrix (vector) transpose operation.

Algorithm 1: Variable Annuity without Early Surrenders via CTMC Approximation-Fast Algorithm

Input: Initialize $\mathbf{Q}^{(m)}$ as in (3.6) and $\mathbf{G}_j^{(N)}$ for $j = 1, 2, \dots, m$, as in (3.12)
 $M \in \mathbb{N}$, the number of time steps,
 $\Delta_M \leftarrow T/M$, the size of a time step

- 1 Set $\mathbf{B}_{j,*} \leftarrow [\varphi(T, e^{x_n + \rho\gamma(v_j)}, v_j)]_{n=1}^N$, $j = 1, 2, \dots, m$
/* Calculate the transition probability matrices */
- 2 **for** $j = 1, 2, \dots, m$ **do**
/* Transition probability matrix of $X^{(m,N)}$ given $V^{(m)} = v_j$ over a period of length Δ_M */
3 $\mathbf{P}_j^X \leftarrow e^{\mathbf{G}_j^{(N)} \Delta_M}$
/* Transition probability matrix of $V^{(m)}$ over a period of length Δ_M */
- 4 $\mathbf{P}^V \leftarrow e^{\mathbf{Q}^{(m)} \Delta_M}$
/* VA valuation */
- 5 **for** $z = M - 1, \dots, 0$ **do**
6 **for** $j = 1, 2, \dots, m$ **do**
7 $\tilde{\mathbf{H}}_{*,j} \leftarrow \mathbf{P}_j^X \mathbf{B}_{j,*}^\top$
8 **for** $n = 1, 2, \dots, N$ **do**
9 $\mathbf{B}_{*,n} \leftarrow \mathbf{P}^V \tilde{\mathbf{H}}_{n,*}^\top$
- 10 **return** b_{ki}

Note that at the end of the last iteration (i.e. when $z = 0$), we have that

$$(4.5) \quad b_{ki} \approx \mathbb{E} \left[e^{-rT} \varphi(T, e^{X_T^{(m,N)} + \rho\gamma(V_T^{(m)})}, V_T^{(m)}) | X_0^{(m,N)} = x_i, V_0^{(m)} = v_k \right].$$

The computational gain of using Algorithm 1 over the previous algorithm comes at the cost of a loss of accuracy since the conditional expectations are approximated over small time intervals (refer to Proposition 4.3). Numerical experiments below show that highly accurate results are obtained in seconds when the time step is small, but the algorithm can perform poorly when the time step is not small enough.

Remark 4.4. *Since at each time step, Algorithm 1, or the “Fast Algorithm”, takes advantage of the tower property of conditional expectations over short time periods of the same length Δ_M , the transition probability matrix can be pre-computed at the beginning of the procedure and stored, accelerating the numerical process greatly. Moreover, as discussed in [24] in the context of option pricing, the method can be used to simultaneously price variable annuities with different guaranteed amounts since the main computational effort in the algorithm resides in the calculation of the matrix exponentials.*

4.2. Variable Annuity with Early Surrenders. We approximate the value of the VA contract (including surrender rights) by its Bermudan counterpart for a large number of monitoring dates. Bermudan options can be exercised early, but only at predetermined dates $R \subset [0, T]$. Thus, Bermudan options are similar to American options, but the region of the permitted exercise times is a subset of $[0, T]$ containing a finite number of exercise dates, $\{t_0, t_1, \dots, t_M\}$ with $t_z \in [0, T]$, $z = 0, 1, 2, \dots, M$ for some $M \in \mathbb{N}$.

In this paper, we use the term Bermudan (resp. American) contract to refer to a variable annuity under which the policyholder has the right to surrender her contract prior to maturity on predetermined dates (resp. at any time prior to maturity). In the same vein, a variable annuity without surrender rights is also called an European contract. Note that these terms do not refer to existing contracts, and they are used to simplify explanations. Naturally, as $M \rightarrow \infty$, we expect the price of the Bermudan contract to converge to the one of a variable annuity with surrender rights as defined in (2.7). The latter is formalized in the following.

Let $\Delta_M = T/M$ for some $M \in \mathbb{N}$ and define the set $\mathcal{H}_M = \{t_0, t_1, \dots, t_M\}$ where $t_z = z\Delta_M$, $z = 0, 1, 2, \dots, M$, so that $t_0 = 0$ and $t_M = T$. The time- t risk-neutral value of the Bermudan contract with permitted exercise dates \mathcal{H}_M is defined by

$$(4.6) \quad b_M(t, x, y) = \sup_{\tau \in \mathcal{T}_{\Delta_M}, \tau \geq t} \mathbb{E}_{t, x, y}[e^{-r(\tau-t)} \varphi(\tau, F_\tau, V_\tau)]$$

where \mathcal{T}_{Δ_M} is the set of stopping times taking values in \mathcal{H}_M . Proposition 4.5 below shows that $b_M(t, x, y) \rightarrow v(t, x, y)$ as $M \rightarrow \infty$.

Proposition 4.5. *As $M \rightarrow \infty$, the value function of the Bermudan variable annuity contract (4.6) converges to its American counterpart (2.7), that is,*

$$\lim_{M \rightarrow \infty} b_M(t, x, y) = v(t, x, y).$$

The proof can be found Appendix A.2.

Remark 4.6. *Using a Bermudan option with a large number of monitoring times to approximate the value of an American option is common in finance; see, for example, [3] and [55]. In fact, since the value of an American option generally does not have closed-form expression, such a time-discretisation is often necessary to implement many numerical techniques.*

In the practical context of variable annuities, surrenders are often only allowed at specific times (such as on the policy anniversary dates). In that case, the Bermudan contract is thus more realistic than its American counterpart in (2.7). Based on this idea, some authors propose numerical procedures which allow for surrenders only at specific points in time, see [66] and [12].

We denote the Bermudan contract value process by $B := \{B_z := b_M(t_z, F_{t_z}, V_{t_z})\}_{0 \leq z \leq M}$. From the principle of dynamic programming (see for example [54], Theorem 10.1.3), it is well-known

that the discretized problem admits the following representation:

$$(4.7) \quad \begin{cases} B_M &= \varphi(T, F_T, V_T) \\ B_z &= \max(\varphi(t_z, F_{t_z}, V_{t_z}), e^{-r\Delta_M} \mathbb{E}_{t_z}[B_{z+1}]), \quad 0 \leq z \leq M-1. \end{cases}$$

Using CTMCs, we can define an approximation for the time- t risk-neutral value of the Bermudan contract by

$$b_M^{(m,N)}(t, x, y) = \sup_{\tau \in \mathcal{T}_{\Delta_M}, \tau \geq t} \mathbb{E} \left[e^{-r\tau} \varphi(\tau, F_\tau^{(m,N)}, V_\tau^{(m)}) | F_t^{(m,N)} = x, V_t^{(m)} = y \right].$$

The approximation of the Bermudan contract value process, denoted by $B^{(m,N)} := \{B_z^{(m,N)} := b_M^{(m,N)}(t_z, F_{t_z}^{(m,N)}, V_{t_z}^{(m)})\}_{0 \leq z \leq M}$, is thus given by

$$(4.8) \quad \begin{cases} B_M^{(m,N)} &= \varphi(T, F_T^{(m,N)}, V_T^{(m)}) \\ B_z^{(m,N)} &= \max(\varphi(t_z, F_{t_z}^{(m,N)}, V_{t_z}^{(m)}), e^{-r\Delta_M} \mathbb{E}_{t_z}[B_{z+1}^{(m,N)}]), \quad 0 \leq z \leq M-1, \end{cases}$$

which can also be written as

$$(4.9) \quad \begin{cases} B_M^{(m,N)} &= \max(G, F_T^{(m,N)}) \\ B_z^{(m,N)} &= \max(g(t, V_t^{(m)}) F_{t_z}^{(m,N)}, e^{-r\Delta_M} \mathbb{E}_{t_z}[B_{z+1}^{(m,N)}]), \quad 0 \leq z \leq M-1. \end{cases}$$

Or equivalently in terms of the process $Y^{(m,N)}$, we have that

$$(4.10) \quad \begin{cases} B_M^{(m,N)} &= \varphi(T, \psi^{-1}(Y_T^{(m,N)})) \\ B_z^{(m,N)} &= \max(\tilde{\varphi}(t_z, \psi^{-1}(Y_{t_z}^{(m,N)})), e^{-r\Delta_M} \mathbb{E}_{t_z}[B_{z+1}^{(m,N)}]), \quad 0 \leq z \leq M-1, \end{cases}$$

where ψ^{-1} is defined in Proposition 3.5¹¹.

Finally, we have $b_M(0, F_0, V_0) = B_0 \approx B_0^{(m,N)} = b_M^{(m,N)}(0, F_0, V_0)$.

Based on the above, an approximation for the value of the Bermudan contract can be obtained as described in the proposition below.

Proposition 4.7. *Let $F_0 > 0$, $V_0 \in \mathcal{S}_V$ and $\mathbf{G}^{(m,N)}$ be the generator defined in (3.14). The risk-neutral value of a variable annuity with maturity $T > 0$ and guaranteed amount $G > 0$ can be approximated recursively by*

$$(4.11) \quad \begin{cases} \mathbf{B}_M^{(m,N)} &= \mathbf{H}^{(1)}, \\ \mathbf{B}_z^{(m,N)} &= \max\{\mathbf{H}_z^{(2)}, e^{-r\Delta_M} \exp\{\Delta_M \mathbf{G}^{(m,N)}\} \mathbf{B}_{z+1}^{(m,N)}\} \quad 0 \leq z \leq M-1, \end{cases}$$

for $M \in \mathbb{N}$ sufficiently large and where the maximum is taken element by element (also known as the parallel maxima). $\mathbf{H}^{(1)}$ and $\mathbf{H}_z^{(2)}$, $z = 0, 1, \dots, M-1$ are column vectors of size $mN \times 1$ whose $(l-1)N + n$ -th entries, $h_{(l-1)N+n}^{(1)}$ and $h_{z,(l-1)N+n}^{(2)}$, are respectively given by

$$(4.12) \quad \begin{cases} h_{(l-1)N+n}^{(1)} &= \max(G, e^{x_n + \rho\gamma(v_l)}), \text{ and} \\ h_{z,(l-1)N+n}^{(2)} &= g(t_z, v_l) e^{x_n + \rho\gamma(v_l)}, \end{cases}$$

$1 \leq l \leq m$ and $1 \leq n \leq N$.

Specifically, given $X_0^{(m,N)} = x_i = \ln(F_0) - \rho\gamma(V_0)$ and $V_0^{(m)} = V_0 = v_k$, the approximated value of the Bermudan contract is given by

$$b_M^{(m,N)}(0, F_0, V_0) = \mathbf{e}_{ik} \mathbf{B}_0^{(m,N)}.$$

Hence, based on the last proposition, Algorithm 2 below provides a CTMC approximation for the value of a variable annuity contract (including early surrenders).

¹¹Recall that $\psi^{-1}(n_y) = (x_n, v_l)$ for $n_y \in \mathcal{S}_Y^{(m,N)}$, where $n \leq N$ is the unique integer such that $n_y = (l-1)N + n$ for some $l \in \{1, 2, \dots, m\}$.

Algorithm 2: Variable Annuity with Early Surrenders via CTMC Approximation

Input: Initialize $\mathbf{G}^{(m,N)}$ as in (3.14), $\mathbf{H}^{(1)}$ and $\mathbf{H}_z^{(2)}$, for $z = 0, 1, \dots, M - 1$, as in (4.12)
 $M \in \mathbb{N}$, the number of time steps,
 $\Delta_M \leftarrow T/M$, the size of a time step

- 1 Set $\mathbf{B}_M^{(m,N)} \leftarrow \mathbf{H}^{(1)}$ and $\mathbf{A}_{\Delta_M} \leftarrow \exp\{\Delta_M \mathbf{G}^{(m,N)}\} e^{-r\Delta_M}$
- 2 **for** $z = M - 1, M - 2, \dots, 0$ **do**
- 3 $\mathbf{B}_z^{(m,N)} \leftarrow \max\{\mathbf{H}_z^{(2)}, \mathbf{A}_{\Delta_M} \mathbf{B}_{z+1}^{(m,N)}\}$
- 4 $b_M^{(m,N)}(0, F_0, V_0) \leftarrow \mathbf{e}_{ik} \mathbf{B}_0^{(m,N)}$
- 5 **return** $b_M^{(m,N)}(0, F_0, V_0)$

Remark 4.8 (Convergence of VA prices with early surrenders). *Recall, from Remark 3.4 that $F^{(m,N)} \Rightarrow F$ as $m, N \rightarrow \infty$. The convergence of the price of the Bermudan contract written on $F^{(m,N)}$ to the price of the Bermudan contract written on F , that is $B_0^{(m,N)} \rightarrow B_0$ as $m, N \rightarrow \infty$, follows from [75], Theorem 9, and the results of [68], Theorem 3.5, on the alternative continuous reward representation of the value function v^{12} . Finally, the convergence of the price of the Bermudan contract to its American counterpart as M goes to infinity follows from Proposition 4.5.*

To our knowledge, detailed error and convergence analysis for the two-layers CTMC approximation of early-exercise options have not yet been performed in the literature. However, [24] demonstrate the accuracy of the approximation numerically in the context of American put option pricing.

4.2.1. *Fast Algorithms.* Algorithm 2, although theoretically correct, might stretch computing resources to unacceptable levels as m, N increase because of the size of the exponent $\mathbf{G}^{(m,N)}$ in the calculation of the matrix exponential (even if the matrix exponential is calculated only once at the beginning of the procedure). However, similarly to the no surrender case, the efficiency of Algorithm 2 can be improved significantly by using an approximation based on the assumption that the variance process remains constant over small time periods (see Proposition 4.3). Indeed, Algorithm 1 can be easily adapted to the valuation of the Bermudan contract since the continuation value in Algorithm 2 is already calculated on a small time interval (thus, it is not necessary to use the tower property of conditional expectations in order to apply the fast methodology.).

Recall that $\mathbf{Q}^{(m)}$ is the generator of $V^{(m)}$, defined in (3.6), and $\mathbf{G}_j^{(N)}$ is the generator of $X^{(m,N)}$ given the variance process is in state v_j , defined in (3.12). Moreover, let $\varphi(t) := [\varphi(t, e^{x_n + \rho\gamma(v_j)}, v_j)]_{j,n=1}^{m,N}$ be a $m \times N$ matrix representing the payoff at time t for each state in $\mathcal{S}_V^{(m)} \times \mathcal{S}_X^{(N)}$, and $\varphi_{j,*}(t)$ be the j -th row of $\varphi(t)$. We denote the matrix (vector) transpose operation by \top .

The Fast Algorithm to value VA with surrender rights is given in Algorithm 3.

The Fast Algorithms to price VA contracts with and without early surrenders are very similar. The only difference is the additional line 11 in Algorithm 3. In fact, at a given time t_z (that is, we fix one z in the loop line 6 to 11), we can observe that at the end of the inner loop (line 9 and 10), the matrix \mathbf{B} contains the continuation value of the Bermudan contract at t_z . Since Bermudan contracts can be surrendered at any time in \mathcal{H}_M , we simply need to calculate the maximum between the continuation value and the payoff at t_z to obtain the value of the Bermudan contract at that time (line 11). Therefore, the only difference between the Fast Algorithms for VA pricing with and without early surrenders stems from the fact that the latter contract cannot be surrendered prior to maturity, and thus, only the continuation value needs to be calculated at each time step (that is, line 11 is not used to price VA contracts without early surrenders).

¹²Many convergence results, such as the one in [75] and [68], require the reward function to be bounded. However, as mentioned in [64], Remark 5.4 and [24], Remark 5, the original payoff φ can be replaced by the truncated payoff $\varphi \wedge L$ with a constant L sufficiently large without altering the accuracy of the numerical results.

Algorithm 3: Variable Annuity with Early Surrenders via CTMC Approximation - Fast Algorithm

Input: Initialize $\mathbf{Q}^{(m)}$ as in (3.6) and $\mathbf{G}_j^{(N)}$ for $j = 1, 2, \dots, m$, as in (3.12)

$M \in \mathbb{N}$, the number of time steps,
 $\Delta_M \leftarrow T/M$, the size of a time step

- 1 Set $\varphi(t_z) \leftarrow [\varphi(t_z, e^{x_n + \rho\gamma(v_j)}, v_j)]_{j,n=1}^{m,N}$ for $z = 0, 1, \dots, M$
- 2 Set $\mathbf{B}_{j,*} \leftarrow \varphi_{j,*}(t_M)$ for $j = 1, 2, \dots, m$
 /* Calculate the transition probability matrices */
- 3 for $j = 1, 2, \dots, m$ do
 /* Transition probability matrix of $X^{(m,N)}$ given $V^{(m)} = v_j$ over a period of length Δ_M */
 /*
 4 $\mathbf{P}_j^X \leftarrow e^{\mathbf{G}_j^{(N)} \Delta_M}$
 /* Transition probability matrix of $V^{(m)}$ over a period of length Δ_M */
- 5 $\mathbf{P}^V \leftarrow e^{\mathbf{Q}^{(m)} \Delta_M}$
 /* VA valuation */
- 6 for $z = M - 1, \dots, 0$ do
- 7 for $j = 1, 2, \dots, m$ do
- 8 $\mathbf{E}_{*,j} \leftarrow \mathbf{P}_j^X \mathbf{B}_{j,*}^\top$
- 9 for $n = 1, 2, \dots, N$ do
- 10 $\mathbf{B}_{*,n} \leftarrow \mathbf{P}^V \mathbf{E}_{n,*}^\top$
- 11 $\mathbf{B} = \max(\mathbf{B}, \varphi(t_z))$
- 12 return b_{ki}

The computational effort in Algorithms 1 and 3 resides in the calculation of the matrix exponentials (line 3 to line 5). Hence, once they are (pre-)computed, one can price variable annuity contracts with and without surrender rights simultaneously at almost no additional cost. This also holds true for any other VA contracts with different guaranteed amount, that is, a large variety of contracts with different guarantee structure and surrender rights can be priced simultaneously for almost the same computational effort as a single contract. Numerical experiments below demonstrate the efficiency and the accuracy of the Fast Algorithm.

4.3. Optimal Surrender Surface. In this section, we provide an algorithm to approximate the optimal surrender strategy for variable annuities with a general fee structure depending on the fund value and the variance process. Policyholder behaviour may significantly impact pricing and hedging of variable annuities, [49]. Thus, analyzing optimal surrender behaviour is crucial for insurers when developing risk management strategies for variable annuities, [67], [7]. Optimal surrender strategies have been studied in the literature in different contexts, see for instance [60], [11], [10], [72] and [46].

The objective is now to approximate the (optimal) surrender surface using the CTMC approximation. To this end, we first introduce some additional definitions and notations.

Definition 4.9. Let $E = [0, T] \times \mathbb{R}_+ \times \mathcal{S}_V$. The continuation region $\mathcal{C} \subset E$ is defined as

$$\mathcal{C} = \{(t, x, y) \in E : v(t, x, y) > \varphi(t, x, y)\},$$

and the surrender region $\mathcal{D} \subseteq E$, as

$$\mathcal{D} = \{(t, x, y) \in E : v(t, x, y) = \varphi(t, x, y)\}.$$

Remark 4.10. It follows from Definition 4.9 that $E = \mathcal{C} \cup \mathcal{D}$, since $v(t, x, y) \geq \varphi(t, x, y)$ for all $(t, x, y) \in E$.

If the value function v is continuous, then \mathcal{C} is an open set and \mathcal{D} is closed; and the optimal surrender surface is the boundary $\partial\mathcal{C}$ of \mathcal{C} .

Definition 4.9 provides a simple way of approximating the optimal surrender surface via CTMC approximation. To do so, denote by f_{nl} the approximated fund process associated to $(x_n, v_l) \in \mathcal{S}_X^{(N)} \times \mathcal{S}_V^{(m)}$ such that $f_{nl} = e^{x_n + \rho\gamma(v_l)}$ and let $\mathcal{S}_F^{(m,N)} = \{f_{nl}\}_{n,l=1}^{N,m}$ be the state-space of $F^{(m,N)}$. We also denote by $\mathcal{S}_{F,l}^{(m,N)} = \{f_{nl}\}_{n=1}^N$ the l -section of $\mathcal{S}_F^{(m,N)}$.

Moreover, let $\tilde{\mathcal{H}}_M = \{t_0, t_1, \dots, t_{m-1}\}$, that is $\tilde{\mathcal{H}}_M = \mathcal{H}_M \setminus t_M$, and $\tilde{E}_l = \tilde{\mathcal{H}}_M \times \mathcal{S}_{F,l}^{(m,N)} \times \{v_l\}$.

Using the previous definitions, the l -section, $l \in \{1, 2, \dots, m\}$, of the continuation and the surrender regions can be approximated using the CTMC processes via

$$\mathcal{C}_l^{(m,N)} = \left\{ (t_z, f_{nl}, v_l) \in \tilde{E}_l \mid b_M^{(m,N)}(t_z, f_{nl}, v_l) > g(t_z, v_l) f_{nl} \right\},$$

and

$$\mathcal{D}_l^{(m,N)} = \left\{ (t_z, f_{nl}, v_l) \in \tilde{E}_l \mid b_M^{(m,N)}(t_z, f_{nl}, v_l) = g(t_z, v_l) f_{nl} \right\} \cup \{T\} \times \mathcal{S}_{F,l}^{(m,N)} \times \{v_l\},$$

respectively. Hence, the approximated continuation and surrender regions are given by

$$\mathcal{C}^{(m,N)} = \cup_{l=1}^m \mathcal{C}_l^{(m,N)}, \quad \text{and} \quad \mathcal{D}^{(m,N)} = \cup_{l=1}^m \mathcal{D}_l^{(m,N)}.$$

We use the notation of Proposition 4.7, with $b_{z,(l-1)N+n}$ denoting the $(l-1)N+n$ -th entry of $\mathbf{B}_z^{(m,N)}$. For (t_z, f_{nl}, v_l) , $0 \leq z \leq M-1$, $1 \leq n \leq N$ and $1 \leq l \leq m$, we set $(t_z, f_{nl}, v_l) \in \mathcal{C}^{(m,N)}$ if $b_{z,(l-1)N+n} > g(t_z, v_l) f_{nl}$, and $(t_z, f_{nl}, v_l) \in \mathcal{D}^{(m,N)}$ otherwise. The approximated optimal surrender surface can then be obtained by analyzing the shape of $\mathcal{C}^{(m,N)}$.

We are now interested in studying the shape of the surrender region. To do so, we fix $t \in [0, T]$ and $y \in \mathcal{S}_V$ and consider the set of points $\mathcal{D}_{t,y} \subseteq \mathbb{R}_+$ for which it is optimal to surrender the contract. More precisely, we define $\mathcal{D}_{t,y}$ by

$$\mathcal{D}_{t,y} = \left\{ f \in \mathbb{R}_+ \mid (t, f, y) \in \mathcal{D} \right\}$$

Suppose that, for all couples $(t, y) \in [0, T] \times \mathcal{S}_V$, the set $\mathcal{D}_{t,y}$ is of the form $[f^*(t, y), \infty)$ for some $f^*(t, y) \in \mathbb{R}_+$. That is, $f^*(t, y)$ is the smallest fund value for which it is optimal to surrender the contract at time t for a volatility level y , and for any fund value greater than $f^*(t, y)$, it is also optimal to surrender. Mathematically, this may be expressed by

$$(4.13) \quad f^*(t, y) := \inf \left\{ f \in \mathbb{R}_+ \mid f \in \mathcal{D}_{t,y} \right\} = \inf \{ \mathcal{D}_{t,y} \}.$$

Under this assumption, the continuation and the surrender regions can be expressed as

$$\mathcal{C} = \left\{ (t, f, y) \in E \mid f < f^*(t, y) \right\},$$

and

$$\mathcal{D} = \left\{ (t, f, y) \in E \mid f \geq f^*(t, y) \right\} \cup \{T\} \times \mathbb{R}_+ \times \mathcal{S}_V,$$

respectively.

Hence, under this assumption, the optimal surrender surface f^* splits E in two regions: at or above the surface is the surrender region, and below, the continuation region. That is, the set $\mathcal{D}_{t,y}$ is connected¹³. In this paper, we say that the surrender region is of ‘‘threshold type’’ if for any $(t, y) \in [0, T] \times \mathcal{S}_V$, the set $\mathcal{D}_{t,y}$ is connected. There is a financial interpretation for such a form for the surrender region. As explained in [65], it is advantageous for the policyholder to hold on to the contract when the fund value is low since there is a higher chance that the guarantee will be triggered at maturity.

¹³A set X is connected if it cannot be divided into two disjoint non-empty open sets.

Remark 4.11. *The surrender region can take any shape; see for examples [61] Figure 4 and Figure 5. However, for specific fee and surrender charge structures, it can be shown that the surrender region is of threshold type, see for instance [60], Appendix 2.A, when the index value process is modelled by a geometric Brownian motion. Other authors take this form for the surrender region as an initial assumption, see for example [46]. In the context of financial derivatives pricing, [44], Proposition 2.1.3, shows that the continuation region of American put options has a threshold type shape under the Black-Scholes setting whereas [77], Section 2, proves it for some stochastic volatility models, and [28], Proposition 4.1, in a very general setting.*

When the surrender region is of threshold type, a simple algorithm can be developed to approximate the optimal surrender surface. The idea is based on the definition of $f^*(t, y)$ in (4.13) above: for each $t_z \in \mathcal{H}_M$ and $v_l \in \mathcal{S}_V^{(m, N)}$, we identify the smallest fund value $f^{(m, N)}(t_z, v_l)$ for which it is optimal to surrender. Algorithm 4 returns the approximated optimal surrender surface $f^{(m, N)}$ (under the assumption that the surrender region is of threshold type) and the approximated value of a variable annuity with early surrenders given $X_0^{(m, N)} = x_i = \ln(F_0) - \rho\gamma(V_0)$ and $V_0^{(m)} = V_0 = v_k$.

Algorithm 4: Optimal Surrender Surface (of threshold type) via CTMC Approximation

Input: Initialize $\mathbf{G}^{(m, N)}$ as in (3.14), $\mathbf{H}^{(1)}$ and $\mathbf{H}_z^{(2)}$, for $z = 0, 1, \dots, M - 1$, as in (4.12)
 $M \in \mathbb{N}$, the number of time steps,
 $\Delta_M \leftarrow T/M$, the size of a time step
1 Set $\mathbf{B}_M^{(m, N)} \leftarrow \mathbf{H}^{(1)}$ and $\mathbf{A}_{\Delta_M} \leftarrow \exp\{\Delta_M \mathbf{G}^{(m, N)}\} e^{-r\Delta_M}$
2 **for** $z = M - 1, M - 2, \dots, 0$ **do**
3 $\mathbf{B}_z^{(m, N)} \leftarrow \max\{\mathbf{H}_z^{(2)}, \mathbf{A}_{\Delta_M} \mathbf{B}_{z+1}^{(m, N)}\}$
4 **for** $l = 1, 2, \dots, m$ **do**
5 $n \leftarrow 1$
6 **while** $(b_{z, (l-1)N+n} > g(t_z, v_l) e^{x_n + \rho\gamma(v_l)})$ **and** $(n < N)$ **do**
7 $n \leftarrow n + 1$
8 $f^{(m, N)}(t_z, v_l) \leftarrow e^{x_n + \rho\gamma(v_l)}$
9 $b_M^{(m, N)}(0, F_0, V_0) \leftarrow \mathbf{e}_{ik} \mathbf{B}_0^{(m, N)}$
10 **return** $f^{(m, N)}$ and $b_M^{(m, N)}(0, F_0, V_0)$

We note that the derivation of the optimal surrender surface is not mandatory to obtain the value of the Bermudan contract, as observed from Algorithm 2 or Algorithm 3 in the previous subsection.

Similarly as above, Algorithm 5 is the fast version of Algorithm 4. Recall that $\mathbf{Q}^{(m)}$ is the generator of $V^{(m)}$ defined in (3.6), $\mathbf{G}_j^{(N)}$ is the generator of $X^{(m, N)}$ given the variance process is in state v_j defined in (3.12), $\varphi(t) := [\varphi(t, e^{x_n + \rho\gamma(v_j)})]_{j, n=1}^{m, N}$ is a $m \times N$ matrix representing the payoff at time t for each state in $\mathcal{S}_V^{(m)} \times \mathcal{S}_X^{(N)}$, and $\varphi_{j, *}(t)$ (resp $\mathbf{B}_{j, *}$) is the j -th row of $\varphi(t)$ (resp. \mathbf{B}). We also denote by b_{jn} , the (j, n) entry of the matrix \mathbf{B} .

Remark 4.12. *Algorithms 2 and 3 do not require the specification of any particular form for the surrender region, which is not the case for many of the numerical procedures presented in the literature ([11],[72] and [46]). Hence their scope is more general.*

The accuracy of the approximated surrender boundary is demonstrated numerically in Appendix B (available online as supplemental material).

4.4. CTMC Approximation of the VIX. In Section 5, we analyze numerically the impact of various VIX-linked fee structure on the optimal surrender strategy. Since analytical formulas for the VIX are not always known for all models listed in Table 1, we use a CTMC approach

Algorithm 5: Optimal Surrender Surface (of threshold type) via CTMC Approximation
 - Fast Algorithm

Input: Initialize $\mathbf{Q}^{(m)}$ as in (3.6) and $\mathbf{G}_j^{(N)}$ for $j = 1, 2, \dots, m$, as in (3.12)
 $M \in \mathbb{N}$, the number of time steps,
 $\Delta_M \leftarrow T/M$, the size of a time step
 1 Set $\varphi(t_z) \leftarrow [\varphi(t_z, e^{x_n + \rho\gamma(v_j)}, v_j)]_{j,n=1}^{m,N}$ for $z = 0, 1, \dots, M$
 2 Set $\mathbf{B}_{j,*} \leftarrow \varphi_{j,*}(t_M)$ for $j = 1, 2, \dots, m$
 /* Calculate the transition probability matrices */
 3 **for** $j = 1, 2, \dots, m$ **do**
 | /* Transition probability matrix of $X^{(m,N)}$ given $V^{(m)} = v_j$ over a period of length Δ_M
 | /*
 4 | $\mathbf{P}_j^X \leftarrow e^{\mathbf{G}_j^{(N)} \Delta_M}$
 | /* Transition probability matrix of $V^{(m)}$ over a period of length Δ_M */
 5 $\mathbf{P}^V \leftarrow e^{\mathbf{Q}^{(m)} \Delta_M}$
 /* VA valuation */
 6 **for** $z = M, M-1, \dots, 0$ **do**
 7 | **for** $j = 1, 2, \dots, m$ **do**
 8 | | $\mathbf{E}_{*,j} \leftarrow \mathbf{P}_j^X \mathbf{B}_{j,*}^\top$
 9 | | **for** $n = 1, 2, \dots, N$ **do**
 10 | | | $\mathbf{B}_{*,n} \leftarrow \mathbf{P}^V \mathbf{E}_{n,*}^\top$
 11 | | $\mathbf{B} = \max(\mathbf{B}, \varphi(t_z))$
 12 | | **for** $j = 1, 2, \dots, m$ **do**
 13 | | | $n \leftarrow 1$
 14 | | | **while** $(b_{jn} > g(t_z, v_j) e^{x_n + \rho\gamma(v_j)})$ **and** $(n < N)$ **do**
 15 | | | | $n \leftarrow n + 1$
 16 | | | $f^{(m,N)}(t_z, v_j) \leftarrow e^{x_n + \rho\gamma(v_j)}$
 17 **return** $f^{(m,N)}$ and b_{ki}

to approximate the value of the volatility index. This is the case for numerical experiments performed under the 3/2 model whose results are available online in Appendix B¹⁴. In this section, we propose an approximation for the VIX when the variance process is approximated by a CTMC.

Let $\{\text{VIX}_t^2\}_{t \geq 0}$ be the process representing the square of the VIX, which is given by

$$\text{VIX}_t^2 = \mathbb{E}_t \left[\frac{1}{\tau} \int_t^{t+\tau} \sigma_S^2(V_s) ds \right],$$

with $\tau = 30/365$, see [26] Equation (6) for details.

Recall that $V^{(m)}$ is the CTMC approximation of V taking values on a finite state-space $\mathcal{S}_V^{(m)} := \{v_1, v_2, \dots, v_m\}$.

When the variance process is a CTMC, a closed-form expression can be obtained for the value of the volatility index. The CTMC approximation of the VIX, denoted by $\text{VIX}^{(m)} = \{\text{VIX}_t^{(m)}\}_{t \geq 0}$, is given in the proposition below.

¹⁴For the 3/2 model, a closed-form expression for the VIX may be found in [18], Theorem 4. However, as pointed out by [31], the integral that appears in the analytical formula is difficult to implement and is not suited for fast and accurate numerical methods. For this reason, the CTMC approximation of the VIX is used in the numerical examples under the 3/2 model.

Proposition 4.13. *Given $V_t^{(m)} = v_k$, the square of the VIX index at time- t can be approximated by*

$$(4.14) \quad \begin{aligned} \left(\text{VIX}_t^{(m),k}\right)^2 &:= \mathbb{E} \left[\frac{1}{\tau} \int_t^{t+\tau} \sigma_S^2(V_s^{(m)}) \, ds \mid V_t^{(m)} = v_k \right] \\ &= \frac{1}{\tau} \int_0^\tau \mathbf{e}_k e^{\mathbf{Q}^{(m)}s} \mathbf{H} \, ds, \end{aligned}$$

where $\tau = 30/365$, $\mathbf{Q}^{(m)}$ is the generator of $V^{(m)}$ defined in (3.6), \mathbf{e}_k is a row vector of size $1 \times m$ with all entries equal to 0 except the k -th entry and \mathbf{H} is a $m \times 1$ vector whose j -th entry h_j is given by $h_j = \sigma_S^2(v_j)$, $j = 1, 2, \dots, m$.

The proof is a direct consequence of Fubini's Theorem and the CTMC representation for conditional expectations.

Remark 4.14. *Because of the time-homogeneity of $V^{(m)}$ the approximation does not depend on t and thus, it needs to be calculated only once for all $t \geq 0$.*

The integral part in (4.14) can be approximated via a quadrature rule. Practically, this is done by dividing the interval $[0, \tau]$ into $n > 0$ equidistant sub-intervals for $z = 0, 1, 2, \dots, n$ with

$$t_z := z\Delta_n, \quad \Delta_n := \tau/n.$$

The approximation then becomes

$$(4.15) \quad \left(\text{VIX}_t^{(m),k}\right)^2 \approx \frac{\Delta_n}{\tau} \mathbf{e}_k \sum_{z=1}^n e^{\mathbf{Q}^{(m)}t_z} \mathbf{H}.$$

Equation (4.15) can be implemented in a straightforward manner. However, it requires calculating the exponential of a matrix n times, which can be computationally inefficient. By making use of the tower property of conditional expectations, Algorithm 6 can be used to speed up the calculation of (4.15).

Algorithm 6: Efficient Algorithm for the calculation of the VIX using CTMC approximation

Input: Initialize $\mathbf{Q}^{(m)}$ as in (3.6) and \mathbf{H} as in Proposition 4.13
 $n \in \mathbb{N}$, the number of time steps,
 $\Delta_n \leftarrow \tau/n$, the size of a time step
1 Set $\mathbf{A}_{\Delta_n} \leftarrow \exp\{\Delta_n \mathbf{Q}^{(m)}\}$, $\mathbf{S} \leftarrow \mathbf{0}_{m \times 1}$ and $\mathbf{E} \leftarrow \mathbf{H}$
2 **for** $z = n, n-1, \dots, 1$ **do**
3 $\mathbf{E} \leftarrow \mathbf{A}_{\Delta_n} \mathbf{E}$
4 $\mathbf{S} \leftarrow \mathbf{S} + \mathbf{E}$
5 $\text{VIX}_t^{(m),k} \leftarrow \sqrt{\mathbf{e}_k \mathbf{S} \frac{\Delta_n}{\tau}}$

The vector $\mathbf{0}_{m \times 1}$ represents the null column vector of size m . Note that Algorithm 6 requires the calculation of a matrix exponential only once at the beginning of the procedure, which makes the algorithm very efficient.

Remark 4.15. *The convergence of the approximation follows easily from the weak convergence of the CTMC approximation (with a reasoning similar to that of Remark 4.2), and the convergence of the time step discretisation, from the monotone convergence theorem.*

Numerical experiments in the next section also demonstrate the accuracy and the efficiency of Algorithm 6 empirically.

5. NUMERICAL ANALYSIS

In the constant fee case, the misalignment between the fees and the value of the financial guarantee creates an incentive for the policyholder to surrender her policy prematurely (see [65] for details). Indeed, when the fund value is high, the amount of the fees paid is also high, but the put option embedded in a GMMB is out-of-the-money and worth very little since the probability for the guarantee to be triggered at maturity is low. Thus, the policyholder pays high fees for a financial guarantee that has a low value. This is clearly an incentive for a policyholder to surrender his policy prior to the term. [61] considered state-dependent fee structures where the fee is paid when the fund value is under a certain level, and showed that this particular type of fee structure reduces insurer's exposure to policyholder behaviour under risk-neutral value maximization assumption. Fees that are tied to the S&P volatility index, VIX, are also studied in the literature, [21], [13] and [50]. Since the volatility is negatively correlated with the stock price (see for instance [69]), we expect VIX-linked fees to be low when the fund value is high and to be higher when the fund value is low. [21] and [50] showed numerically that linking the fee to the volatility index VIX may help realign revenues with variable annuity liabilities (for VA without surrender rights). Hence, it is normal to believe that linking the fees to the VIX may help to reduce insurers' exposure to surrender risk. This will be explored in greater details in the numerical experiments conducted below.

This section first discusses the market, the VA, and the CTMC parameters used in all numerical experiments performed below. Then, we investigate the efficiency of the Fast Algorithms (Algorithms 1 and 3). In the third subsection, we discuss different structures for the VIX-linked fee, that is, different ways to link the fee rate to the VIX index. Finally, we analyze the impact of different VIX-linked fee structures on the value of VAs and their optimal surrender strategy. We restrict our analysis to the classical Heston model. Using our framework, any model listed in Table 1 could have been used.

As supplementary material (available online), we investigate the numerical accuracy of the approximated optimal surrender surface derived in Algorithm 4 (or equivalently 5), and the CTMC approximation of the VIX (Algorithm 6). Finally, we explore numerically the impact of VIX-linked fee structures under the 3/2 model.

5.1. Market, VA and CTMC Parameters. We consider a market under regular conditions: low initial variance v_0 , low long-term variance θ , moderate volatility of volatility σ , and moderate speed reversion κ ¹⁵. The initial value of the variance is set to $V_0 = 0.03$, the correlation to $\rho = -0.75$ and the risk-free rate to $r = 0.03$. The selected market parameters are summarized in Table 2 and the model dynamic is given in Table 1.

Parameter	V_0	κ	θ	σ	ρ	r
Value	0.03	2.00	0.04	0.20	-0.75	0.03

TABLE 2. Market Parameters

The variable annuity parameters are set to $F_0 = S_0 = 100$, $T = 10$ (years), and $G = 100$. We assume that the payoff when the contract is surrendered early is given by $g(t, V_t)F_t$, with

$$g(t, y) = e^{-k(T-t)}, \quad y \in \mathcal{S}_V,$$

and $k = 0.2\%$. As mentioned previously, such a form for the early surrender payoff is common in the actuarial literature, see [11], [60], [10],[61], [72], [5] and [46]. The choices for the fee function $c(x, y)$ are discussed in greater details in the next section.

¹⁵Bloomberg provides historical Heston calibrated parameters to market data on a daily basis via its Option Pricing template (OVME). These parameters are currently used in practice for over-the-counter option pricing. Bloomberg's Heston calibrated speed reversion parameter is $\kappa = 3.6881$ as of December 31, 2019, $\kappa = 5$ as of March 31, 2020 and $\kappa = 1.1397$ as of September 30, 2020. The parameter selected for our numerical experiments falls approximately in the middle of those of December 2019 and September 2020. In the financial literature, [1] obtain $\kappa = 5.07$ whereas [35] obtain $\kappa = 0.173$, and again our values fall between these two values.

Note that a numerical analysis under the Heston model with $G = F_0 e^{\tilde{g}T}$, $\tilde{g} = 2\%$ (rather than $G = 100$) is also performed in Appendix B, available online as supplemental material.

For all numerical examples in this paper, we use the non-uniform grid proposed by Tavella and Randall ([76], Chapter 5.3). For example, suppose that \tilde{X} is a one-dimensional diffusion process approximated by a continuous-time Markov chain $\tilde{X}^{(n)}$ taking values on a finite state-space $\mathcal{S}_{\tilde{X}} = \{\tilde{x}_1, \tilde{x}_2, \dots, \tilde{x}_n\}$, $n \in \mathbb{N}$. The state-space of the approximated process can be determined as follows:

$$(5.1) \quad \tilde{x}_i = \tilde{X}_0 + \tilde{\alpha} \sinh \left(c_2 \frac{i}{m} + c_1 \left[1 - \frac{i}{m} \right] \right), \quad i = 2, \dots, m-1,$$

where

$$c_1 = \sinh^{-1} \left(\frac{\tilde{x}_1 - \tilde{X}_0}{\tilde{\alpha}} \right), \quad \text{and} \quad c_2 = \sinh^{-1} \left(\frac{\tilde{x}_m - \tilde{X}_0}{\tilde{\alpha}} \right).$$

Here the constant, $\tilde{\alpha} \geq 0$, controls the degree of non-uniformity of the grid. When $\tilde{\alpha}$ is small, we obtain a highly non-uniform grid with more points concentrated around X_0 , whereas the grid is uniform for high values of $\tilde{\alpha}$. The choices for the two boundary states and the non-uniformity parameter $\tilde{\alpha}_v$ (resp. $\tilde{\alpha}_X$) for $V^{(m)}$ (resp. $X^{(m,N)}$) are discussed in more details below.

Remark 5.1. *When the initial values of the auxiliary and variance processes are not in the grid, they can be inserted (see for example [25], Section 2.3 for details), or the value of the variable annuity must be interpolated between the appropriate grid points.*

Non-uniform schemes have been used frequently in the literature for options pricing via CTMC approximation methods, see [64], [57], [16], [48], [56],[24], [25] and [58], among others. It has also been used for solving partial differential equations (PDEs) numerically, see for instance [76]. [57] showed numerically that non-uniform grids are more stable and can converge faster than uniform grids. In the equidistant grid setting, the choice of boundary values significantly impacts the convergence to the true option price. Also, appropriate bounds depend on the parameters of the underlying process and the maturity of the option, and thus, may be difficult to find. [56] tested four different schemes to approximate the volatility process in the Heston model. They conclude that the grid proposed by Tavella and Randall (5.1) is the most robust and precise in general, whereas the method proposed by [64], Section 4, requires few Markov states to achieve good accuracy. For a deep analysis of grid designs and how they can affect convergence, the reader is referred to [80].

Unless stated otherwise, all numerical experiments are performed using the CTMC parameters listed in Table 3. Recall that m is the number of grid points for the variance process whereas N represents the number of grid points of the fund process. $\tilde{\alpha}_v$ (resp. $\tilde{\alpha}_X$) is the grid non-uniformity parameter of the variance (resp. the auxiliary) process. The grid's upper and lower bounds are respectively v_1 and v_m for the variance process and x_1 and x_N for the auxiliary process with $X_0 = \ln(F_0) - \rho\gamma(V_0)$. The values of V_0 and X_0 are inserted in their respective grid as per Remark 5.1. Finally, we use $M = 500 \times 10$ times steps, which corresponds to a computing frequency of approximately twice daily (since there are approximately 250 trading days per year).

Parameter	m	N	v_1	v_m	$\tilde{\alpha}_v$	x_1	x_N	$\tilde{\alpha}_X$	M
Value	50	2,000	$V_0/100$	$7v_0$	0.6571	$X_0/10^6$	$1.95X_0$	2/100	5,000

TABLE 3. CTMC Parameters

Note that, under the Heston model, good approximations of the transition density of the variance process can be obtained with a small number of grid points, see for example [25] Figure 3. All the numerical experiments are carried out with Matlab R2015a on a Core i7 desktop with 16GM RAM and speed 2.40 GHz.

5.2. Efficiency of the Fast Algorithms. The valuation of options (or variable annuities) using CTMC requires the calculation of a matrix exponential to obtain the transition probability matrix. In Algorithm 2, the two-dimensional process is mapped onto a one-dimensional process resulting in a generator of size $mN \times mN$. Thus, we need to calculate the exponential of a $mN \times mN$ matrix to obtain the transition probability matrix. For large values of mN , this procedure might stretch computing resources to unacceptable levels. Algorithms 1 and 3, proposed in Section 4, require m times the calculation of the exponential of a $N \times N$ matrix and one time the exponential of a $m \times m$ matrix. As demonstrated below, reducing the size of the matrix in the exponent allows to significantly increase the efficiency of the procedure.

When the size of the exponent in the matrix exponential is greater than 200×200 , we observe that the function *fastExpm* for Matlab, see [62]¹⁶, which is designed for the fast calculation of matrix exponentials of large sparse matrices, can further speed up the calculation. Combining the function *fastExpm* and the Fast Algorithms can speed up the code by up to 100 times (for European and Bermudan contracts). For the European contract, the Fast Algorithm can decrease the running time by up to 12 times whereas the function *fastExpm*, by up to 7 times. For the Bermudan contract, the computation time is decreased by up to 4 times with the Fast Algorithm and by up to 40 times with the function *fastExpm*. When $m = 50$ and $N = 100$ the running time is approximately 6 seconds for both the European and the Bermudan contracts, confirming the high efficiency of the new algorithms. Figure 1 illustrates the computation time in seconds of the “Fast Algorithm”, Algorithm 1 for the European contract and Algorithm 3 for the Bermudan contract, combined with the function *fastExpm* of [62] (when the size of the generator in the matrix exponential is greater than 200×200), and the computation time of the “Regular Algorithm” for the European contract (4.2) and Algorithm 2 for the Bermudan one. The running time in Figure 1 are recorded using market, VA and CTMC parameters of Subsection 5.1; except for the number of grid points for the auxiliary process N which is set to $N = 100, 200, 300$ and 500 , respectively. Moreover, we use a constant fee structure, that is we fix $c(x, y) = 1.5338\%$ for all $(x, y) \in \mathbb{R}_+ \times \mathcal{S}_V$.

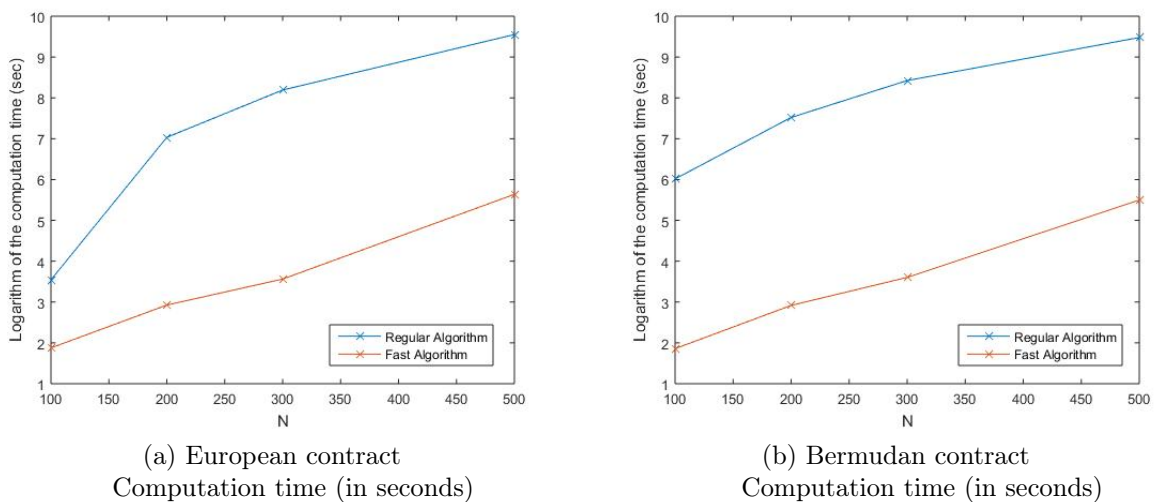


FIGURE 1. Fast Algorithms: Algorithm 1 for the European contract and Algorithm 3 for the Bermudan contract. Regular Algorithms: Equation (4.2) for the European contract and Algorithm 2 for the Bermudan contract.

We also compare the accuracy of the new algorithms. For comparison, we use the regular algorithms for the European contract and for the Bermudan contract. The absolute difference in the

¹⁶The function *fastExpm* is based on [42] and [51].

VA prices between the regular and the fast algorithms is around 10^{-3} for both European and Bermudan contracts, whereas the relative difference is around 10^{-5} , confirming the accuracy of the fast algorithms. See also Appendix (B) available online for more details.

Remark 5.2. *When valuing a European contract, the use of the Expokit of [73] based on Krylov subspace projection methods accelerates the computation time considerably. Moreover, software packages in Matlab and Fortran can be downloaded for free at <https://www.maths.uq.edu.au/expokit>. When $N = 500$, we observe that the function `expv` in the Expokit can accelerate the running time by up to 7 times (compared to the fast algorithm).*

However, since the function takes advantage of the product of a matrix exponential with a vector, the fast algorithm is more efficient when valuing Bermudan contract. Indeed, when using the fast algorithm, matrix exponentials are calculated only once at the beginning of the procedure; whereas when using the Expokit, it needs to be calculated at each time step (since we need to calculate the matrix exponential multiplied by a vector in order to make use of the procedure) which slows down the execution considerably. Hence, when valuing a Bermudan contract, Algorithm 3 is up to 9 times faster than the regular algorithm using Expokit procedures of [73].

As mentioned previously, the computational effort in Algorithms 1 and 3 resides in the calculation of the matrix exponentials at the beginning of the two procedures. Hence, once they are (pre-)computed, one can obtain the value of variable annuities with and without surrender rights simultaneously at almost no additional cost. For instance, when $N = 500$, we simultaneously obtain the prices of variable annuities with and without surrender rights in 270 seconds; whereas the values of the Bermudan and the European contracts can be obtained separately in approximately 250 seconds for each. This also holds true for any other VA contracts with different guaranteed amounts; that is, a variety of contracts can be priced for almost the same computational effort as a single contract.

5.3. Fee Structures and Fair Fee Parameters. First, recall from Subsection 4.4 that

$$\text{VIX}_t^2 = \mathbb{E}_t \left[\frac{1}{\tau} \int_t^{t+\tau} \sigma_S^2(V_s) ds \right], \quad \text{with } \tau = 30/365.$$

For all the numerical experiments conducted below, we consider three types of VIX-linked fee structures. As in [21], we use an uncapped VIX²-linked fee structure (the ‘‘Uncapped VIX²’’ fee structure) of the form

$$c_t = \tilde{c} + \tilde{m} \text{VIX}_t^2, \quad 0 \leq t \leq T,$$

with $\tilde{c}, \tilde{m} \geq 0$.

When the volatility is high (e.g. financial turmoil), the Uncapped VIX² fee rate can become excessive (see Table 5 for examples). Thus, as mentioned in [21], it may be interesting to introduce a cap to the actual VIX²-linked fee structure in order to keep the product marketable and to reduce the negative net return on the VA account resulting from a high fee. This motivates our choice of imposing a cap to this type of fee.

Thus, for the second fee structure, we consider capped VIX²-linked fees (or simply the ‘‘Capped VIX²’’ fee structure or Capped fee structure) of the form

$$c_t = \min(\tilde{c} + \tilde{m} \text{VIX}_t^2, K), \quad 0 \leq t \leq T,$$

where $\tilde{c}, \tilde{m} \geq 0$ and $K > 0$.

Finally, we look at an uncapped fee structure linked to the VIX (rather than the VIX squared), also called the ‘‘Uncapped VIX’’ fee structure. Such a structure can help to keep the fee rates reasonable during high volatility periods. More precisely, we consider a third fee process of the form

$$c_t = \tilde{c} + \tilde{m} \text{VIX}_t, \quad 0 \leq t \leq T,$$

with $\tilde{c}, \tilde{m} \geq 0$.

Since the volatility process is Markovian, the volatility index at t will depend only on V_t . Therefore, the three fee functions are of the form $c(y)$, $y \in \mathcal{S}_V$.

Analytical formulas for the VIX are not known for all the models stated in Table 1. In that case, CTMCs can be used to approximate the value of the volatility index as discussed in Subsection 4.4.

The fee structure parameters \tilde{c} and \tilde{m} are set in such a way that the contract is fair at inception. That is, the initial amount invested by the policyholder, F_0 , is equal to the expected discounted value of the future benefit (without early surrenders). Those parameters are called the fair parameters and are henceforth denoted by a star: $(\tilde{c}^*, \tilde{m}^*)$. We set the fee in this manner to calculate the value added by the right to surrender. To identify the fair fee vector $(\tilde{c}^*, \tilde{m}^*)$, we first fix a multiplier \tilde{m}^* , and then solve for the corresponding fair base fee \tilde{c}^* . Note that such a fair base fee \tilde{c}^* does not exist for all values of $\tilde{m}^* > 0$. When $c_t = \tilde{c}^* + \tilde{m}^* \text{VIX}_t^2$, the fair parameters are obtained using the exact formula of [21]. For the other fee structures, the fair parameters are calibrated using a CTMC approximation with $N = 100$ (all other CTMC parameters are the same as in Table 3), to reduce the computation time. Note that very accurate VA prices are obtained extremely fast with $N = 100$ under the Heston model, see Appendix B, available online, for numerical details. Table 4 presents the fair fee vectors $(\tilde{c}^*, \tilde{m}^*)$, and Table 5 shows examples of fair fee rates produced by each fair fee vector at different volatility levels $(\sqrt{V_t})^{17}$.

	$c_t = \tilde{c}^* + \tilde{m}^* \text{VIX}_t^2$			
\tilde{m}^*	0.0000	0.1500	0.3000	0.4345
\tilde{c}^*	1.5338%	1.0036%	0.4741%	0.000%
	$c_t = \min\{\tilde{c}^* + \tilde{m}^* \text{VIX}_t^2, K\}, K = 2\%$			
\tilde{m}^*	0.0000	0.1500	0.3000	0.4927
\tilde{c}^*	1.5338%	1.0112%	0.5415%	0.000%
	$c_t = \tilde{c}^* + \tilde{m}^* \text{VIX}_t$			
\tilde{m}^*	0.0000	0.0250	0.0500	0.0836
\tilde{c}^*	1.5338%	1.0750%	0.6164%	0.000%

TABLE 4. Fair fee vectors $(\tilde{c}^*, \tilde{m}^*)$

The uncapped VIX^2 -linked fee rate can get very high as the volatility increases, reaching levels as high as 7.4653% when the volatility is 42.772%. During the last COVID-19 financial crisis, volatility reached levels as high as 80% in March 2020¹⁸. This motivates the two other fee structures we propose. The introduction of a cap does not significantly affect the calibrated fair fee parameters. For instance, when $\tilde{m}^* = 0.3$, the calibrated base fee rate jumps slightly from $\tilde{c}^* = 0.4741\%$ to $\tilde{c}^* = 0.5415\%$ when the cap is included, and when $\tilde{c}^* = 0.0000\%$, the fair multiplier goes from $\tilde{m}^* = 0.4345$ to $\tilde{m}^* = 0.4927$. The other fair fee vectors are almost the same under both structures. However, when we compare Tables 5 (A) and (B), we observe that the introduction of such a cap allows to keep the product marketable by avoiding excessive fee rates during financial turmoil. Comparing Tables 5 (A) and (C), we note that fee rates of the VIX fee structure are slightly higher during low/regular volatility periods than the ones of the VIX^2 fee structure. This slight increase in fee rates in low volatility regimes allows the fees to be kept at reasonable levels during high volatility periods compared to the Uncapped VIX^2 fee structure. Thus, this third uncapped fee function is also clearly more attractive from the policyholder's perspective.

¹⁷Under the Heston model there is a closed-form expression for the VIX given by $\text{VIX}_t^2 = B + AV_t$ with $A = \frac{1 - e^{-\kappa\tau}}{\kappa\tau}$ and $B = \frac{\theta(\kappa\tau - 1 + e^{-\kappa\tau})}{\kappa\tau}$, see [81].

¹⁸See VIX historical data at https://www.cboe.com/tradable_products/vix/vix_historical_data/.

$\sqrt{V_t}$ (%) \ \tilde{m}^*	0.0000	0.1500	0.3000	0.4345
8.702	1.5338	1.1550	0.7770	0.4387
13.882	1.5338	1.3168	1.1007	0.9075
30.434	1.5338	2.3314	3.1299	3.8464
42.772	1.5338	3.5808	5.6285	7.4653

(A) $c_t = \tilde{c}^* + \tilde{m}^* \text{VIX}_t^2$ (%)

$\sqrt{V_t}$ (%) \ \tilde{m}^*	0.0000	0.1500	0.3000	0.4927
8.702	1.5338	1.1627	0.8444	0.4975
13.882	1.5338	1.3245	1.1681	1.0291
30.434	1.5338	2.0000	2.0000	2.0000
42.772	1.5338	2.0000	2.0000	2.0000

(B) $c_t = \min\{\tilde{c}^* + \tilde{m}^* \text{VIX}_t^2(\%), K\}$, $K = 2\%$

\sqrt{y} (%) \ \tilde{m}^*	0.0000	0.0250	0.0500	0.0836
8.702	1.5338	1.3262	1.1188	0.8402
13.882	1.5338	1.4363	1.3390	1.2083
30.434	1.5338	1.8188	2.1041	2.4877
42.772	1.5338	2.1113	2.6889	3.4657

(C) $c_t = \tilde{c}^* + \tilde{m}^* \text{VIX}_t$

TABLE 5. Fair fee rates in %

5.4. **Effect of VIX-Linked Fees on Surrender Incentives.** Recall that under the Heston model, [40], the price of the risky asset satisfies

$$(5.2) \quad \begin{aligned} dS_t &= rS_t dt + \sqrt{V_t} S_t dW_t^{(1)} \\ dV_t &= \kappa(\theta - V_t) dt + \sigma \sqrt{V_t} dW_t^{(2)}, \end{aligned}$$

with S_0 and V_0 are deterministic, and where $W = (W^{(1)}, W^{(2)})^T$ is a bi-dimensional correlated Brownian motion under \mathbb{Q} and such that $[W^{(1)}, W^{(2)}]_t = \rho t$ with $\rho \in [-1, 1]$, the speed of the mean-reversion $\kappa > 0$, the long term variance $\theta > 0$ and the volatility of the variance $\sigma > 0$ (also called the volatility of the volatility).

Moreover, when the market is modeled by (5.2), the VIX has a closed-form expression given by

$$(5.3) \quad \text{VIX}_t^2 = B + AV_t$$

with $A = \frac{1-e^{-\kappa\tau}}{\kappa\tau}$ and $B = \frac{\theta(\kappa\tau-1+e^{-\kappa\tau})}{\kappa\tau}$, see [81] for details.

The three fee structures exposed in the Subsection 5.3 can thus be obtained explicitly in terms of the current volatility using (5.3) as follows:

Fee Structure	$c_t, 0 \leq t \leq T$
Uncapped VIX²	$c_t = \tilde{c}^* + \tilde{m}^*(A + BV_t)$
Capped VIX²	$c_t = \min\{K, \tilde{c}^* + \tilde{m}^*(A + BV_t)\}$
Uncapped VIX	$c_t = \tilde{c}^* + \tilde{m}^* \sqrt{(A + BV_t)}$

TABLE 6. Fair fee process under the Heston model

Now from Lemma 3.3, we find that $\gamma(x) = x/\sigma$. Thus, given a certain fee process c_t (listed in Table 6), the dynamics of the auxiliary process can be derived as

$$(5.4) \quad \begin{aligned} dX_t &= \mu_X(X_t, V_t) dt + \sigma_X(V_t) dW_t^*, \\ dV_t &= \mu_V(V_t) dt + \sigma_V(V_t) dW_t^{(2)}, \end{aligned}$$

where $\mu_X(X_t, V_t) = r - \frac{\rho\kappa\theta}{\sigma} - c_t + V_t \left(\frac{\rho\kappa}{\sigma} - \frac{1}{2} \right)$, and $\sigma_X(V_t) = \sqrt{(1 - \rho^2)V_t}$, $0 \leq t \leq T$.

Using the CTMC technique outlined in Section 3 and the market, VA, and CTMC parameters of subsection 5.1, we perform the valuation of a variable annuity with and without early surrenders (“VA with ES” and “VA without ES”, respectively). The results are reported in Table 7 below¹⁹.

$\tilde{m}^* =$	0.0000	0.1500	0.3000	0.4345
$\tilde{c}^* =$	1.5338%	1.0036%	0.4741%	0.000%
VA without ES	100.00090	100.00091	100.00092	100.00093
VA with ES	103.01785	103.00823	103.00330	103.00367
Value of ES	3.01695	3.00732	3.00238	3.00274
(A) $c_t = \tilde{c}^* + \tilde{m}^* \text{VIX}_t^2$				
$\tilde{m}^* =$	0.0000	0.1500	0.3000	0.4927
$\tilde{c}^* =$	1.5338%	1.0112%	0.5415%	0.000%
VA without ES	100.00090	100.00075	100.00070	100.00036
VA with ES	103.01785	103.00596	102.99137	102.97560
Value of ES	3.01695	3.00521	2.99067	2.97524
(B) $c_t = \min\{K, \tilde{c}^* + \tilde{m}^* \text{VIX}_t^2\}$, with $K = 2\%$				
$\tilde{m}^* =$	0.0000	0.0250	0.0500	0.0.0836
$\tilde{c}^* =$	1.5338%	1.0750%	0.6164%	0.000%
VA without ES	100.00090	100.00099	100.00057	100.000167
VA with ES	103.01785	103.01080	103.00446	102.99853
Value of ES	3.01695	3.00981	3.00389	2.99686
(C) $c_t = \tilde{c}^* + \tilde{m}^* \text{VIX}_t$				

TABLE 7. Variable annuity with and without early surrender (ES).

First, we observe that the fair value of the variable annuity without early surrenders is approximately $F_0 = 100$ for all fair fee vectors. This is because fair fee parameters are calibrated such that the value of the VA without surrender rights at time $t = 0$ is equal to the initial premium ($F_0 = 100$). Moreover, under the Uncapped VIX²-linked structure, fair fee parameters are obtained using the exact pricing formula of [21], confirming the accuracy of the approximated model. The absolute error is around 10^{-4} for all fee vectors for this fee structure. An accuracy around 10^{-3} can be obtained for each value (the value of the VA with and without surrender rights) with fewer grid points with significantly less computational effort. Detailed results with $N = 100$ and $N = 1,000$ are given in Appendix B (available online as supplemental material) with their respective computation time. The value of the surrender right is calculated as the difference between the values of the variable annuity with and without early surrenders.

As \tilde{m}^* increases, the risk-neutral value of early surrenders remains almost the same for all fee structures. We were expecting a VIX-linked fee structure to reduce the risk-neutral value of the surrender rights since this type of fee structure realigns income and liability, [21], but this is not what we observe here. However, VIX-linked fee structures have an impact on optimal surrender strategies, as shown below.

In Figure 2, the shape of the approximated optimal surrender surface associated to each of the VIX-linked fee structure is illustrated for different values of the fair multiplier. We observe that

¹⁹Numerical experiments under the Heston model have been performed using Equation (4.2), and Algorithms 2 and 4. Note however that similar results are obtained when using the Fast Algorithms, see Appendix B, available online for details.

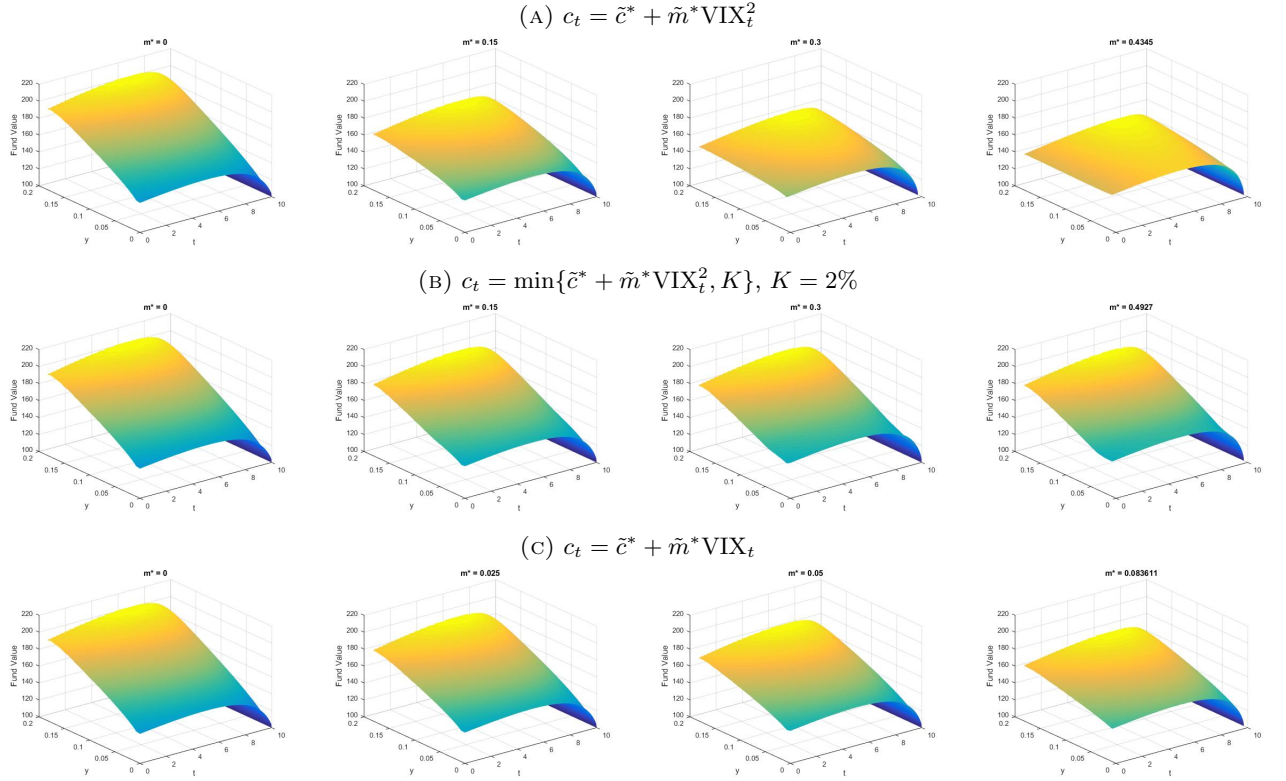


FIGURE 2. Approximated optimal surrender surface of VIX-linked fees VAs for different values of fair multiplier \tilde{m}^* under the Heston model. The x -axis represents the time and the y -axis the variance.

the surrender region is of threshold type for all \tilde{m}^* . We also note that, regardless of the value of \tilde{m}^* , the boundary is a concave function in the time variable. It slowly increases to a maximum and decreases rapidly to the guarantee level G . This is consistent with earlier findings of [11] and [46].

Now fix $t \in [0, T]$ and observe, in Figures 2 and 3, that the t section of $f^{(m, N)}$, the function $y \mapsto f^{(m, N)}(t, y)$, denoted by $f_t^{(m, N)}$, is increasing for all \tilde{m}^* . Hence, when the volatility is high, variable annuities are surrendered for higher fund values in contrast to low volatility levels. This is in line with findings of [46]. However, as \tilde{m}^* increases, the function $f_t^{(m, N)}$ increases more slowly (and particularly for the uncapped structures, panel (A) and (C) of Figures 2 and 3). For instance, fix $\tilde{m}^* \in \{0, 0.15, 0.3, 0.4345\}$, $y \in \mathcal{S}_V^{(m)}$ and note, from Figure 3 (panel (A) or (C)), that the y section of $f^{(m, N)}$, the function $t \mapsto f^{(m, N)}(t, y)$, denoted by $f_y^{(m, N)}$, is pushed upwards as y increases. However, the difference between the low and the high volatility y section is less significant as \tilde{m}^* grows. This means that the optimal surrender decision for uncapped VIX-linked fees is less sensitive to volatility fluctuations when fees are tied to the volatility index. When we look at the capped structure (panel (B) of Figures 2 and 3), we also note that approximated optimal surrender surfaces are gradually increasing as volatility grows; however, they now increase at essentially almost all the same pace for all \tilde{m}^* . This can be interpreted from a financial perspective as pointed out below.

In Figure 4, we fix a volatility level y and we compare the y sections of $f^{(m, N)}$, $f_y^{(m, N)}$, for different fair multipliers \tilde{m}^* . When the volatility is low ($\sqrt{y} = 8.702\%$), see for instance the first graph of Figure 4 (A), we observe that $f_y^{(m, N)}$ is pushed upwards with increasing values of \tilde{m}^* . This means that a variable annuity contract with a fully dependent uncapped VIX²-linked fee structure

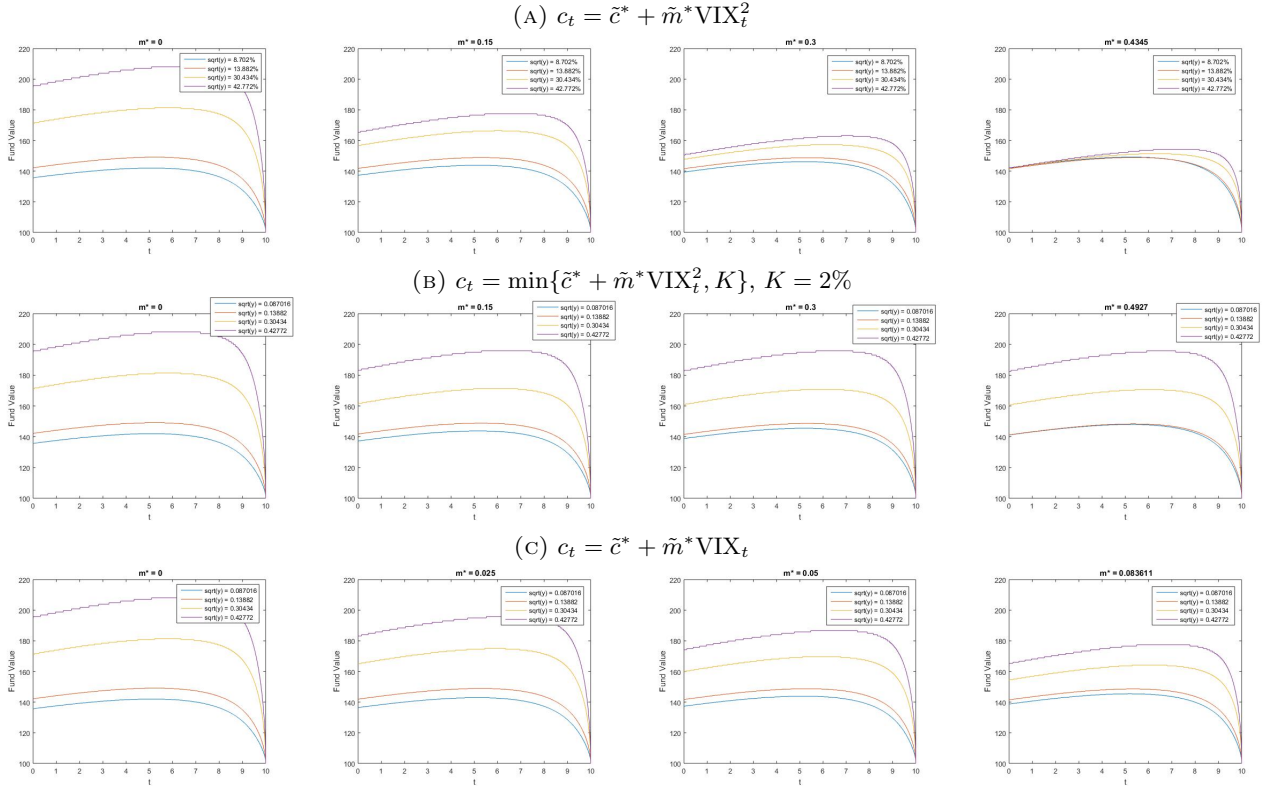


FIGURE 3. The y section of the approximated optimal surrender surface, $f_y^{(m,N)}$, for different volatility levels \sqrt{y} and fair multipliers \tilde{m}^* .

($\tilde{m}^* = 0.4345$) is surrendered at higher fund values than the constant fee one ($\tilde{m}^* = 0$). Indeed, when the volatility is low, the fee paid under a variable annuity contract with a VIX²-linked fee structure is also low (see Table 5 for examples), making VIX-linked fee contracts more attractive than the constant fee ones. However, as the volatility rises, VIX²-linked fees also rise and so, the relation between the optimal surrender decision and \tilde{m}^* reverts. The second graph of Figure 4 (A) shows that variable annuity contracts are surrendered at almost all the same fund value levels when the volatility equals to 13.882%, regardless of m^* . The latter may be explained by the fact that fee rates are all around the same level when $\sqrt{y} = 13.882\%$, that is $\pm 1\%$ as per Table 5. However, when the volatility increases (see for instance the third and the last graphs of Figure 4 (A)), VIX²-linked fees are also high (refer again to Table 5 for examples), making VIX²-linked fee variable annuity contracts less attractive than the constant fee ones. And so, when volatility is high, we observe that $f_y^{(m,N)}$ is pushed downward with increasing values of \tilde{m}^* . Or, in other words, for high volatility levels, variable annuity contracts with VIX²-linked fee structures are surrendered for fund values that are less than the ones with constant fee structures. This is financially intuitive, as pointed out by [11] under the Black-Scholes setting with a constant fee function, since when the fee gets higher, the policyholder has to pay more for the guarantee, and so, the mismatch between the premium for guarantee and its value is even greater; resulting in earlier exercise time. The analysis above shows that the findings of [11] also extends to stochastic fee structures. Similar conclusion can be drawn for the Uncapped VIX-linked fees, Figure 4(C).

For the capped fees, we observe in Figure 4(B) that when the volatility is low, capped VIX²-linked fee VA contracts are surrendered for lower fund value than the constant fee ones, as for the two other fee structures. However, when the volatility gets high enough, the cap is reached, and so, the fee paid under the capped structure is the same for all $m^* > 0$ (see Table 5); the capped

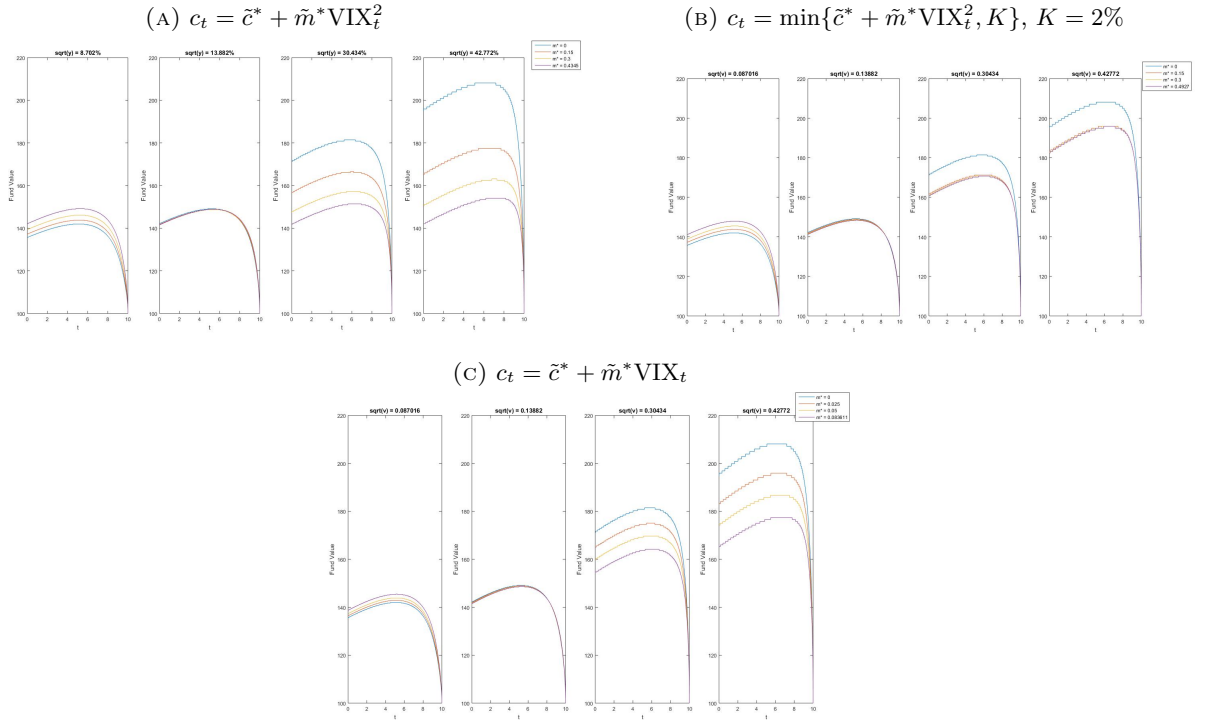


FIGURE 4. The y section of the approximated optimal surrender surface, $f_y^{(m,N)}$, for different volatility levels \sqrt{y} and fair multipliers \tilde{m}^* .

VIX²-linked fee VA contracts are thus surrendered at almost all the same fund value level (Figure 4 (B) graphs 3 and 4 when $m^* > 0$). This illustrates again the relation that exists between fees and optimal surrender decisions. VA contracts with higher fee rates are surrendered for lower fund values than contracts with lower fee rates.

Similar conclusions can be drawn when $G = F_0 e^{\tilde{g}T}$ with $\tilde{g} = 2\%$ in the Heston model and under the 3/2 stochastic volatility model, see Appendix B, available online as supplemental material, for details.

6. CONCLUSION

In this paper, we provide a framework based on CTMC approximations to analyze the surrender incentives resulting from VIX-linked fees in variable annuities under general stochastic volatility models. Under the assumption that the policyholder will maximize the risk-neutral value of his variable annuity, the pricing of a variable annuity is an optimal stopping problem with a time-discontinuous reward function. Under general fee and surrender charge structures, we develop efficient numerical algorithms based on a two-layers CTMC approximation to price variable annuities with and without early surrenders. We derive a closed-form analytical formula for the value of a variable annuity without surrender rights and provide a quick and simple way of determining early surrenders value via a recursive algorithm. We also present an easy procedure to approximate the optimal surrender surface under the hypothesis that the surrender region is of threshold type. Lastly, we observe numerically that VIX-linked fees do not significantly affect the value of early surrenders under the selected set of Heston parameters. However, numerical examples also reveal that the optimal surrender decision is impacted by VIX-linked fee structures. In particular, we observe that the optimal surrender strategy is more stable with respect to volatility changes when the fees are linked to the volatility index. The CTMC approximation of the VIX presented

in Section 4.4 can also be used to price exotic path-dependent options on the VIX, which is left as future research.

DISCLOSURE STATEMENT

The authors report there are no competing interests to declare.

REFERENCES

- [1] Yacine Aït-Sahalia and Robert Kimmel, *Maximum likelihood estimation of stochastic volatility models*, Journal of Financial Economics **83** (2007), no. 2, 413–452.
- [2] Jennifer Alonso-García, Michael Sherris, Samuel Thirurajah, and Jonathan Ziveyi, *Taxation and Policyholder Behavior: The case of Guaranteed Minimum Accumulation Benefits*, Available at SSRN 3629101 (2021).
- [3] Kaushik Amin and Ajay Khanna, *Convergence of American option values from discrete-to continuous-time Financial models*, Mathematical Finance **4** (1994), no. 4, 289–304.
- [4] Anna Rita Bacinello, Pietro Millosovich, Annamaria Olivieri, and Ermanno Pitacco, *Variable annuities: A unifying valuation approach*, Insurance: Mathematics and Economics **49** (2011), no. 3, 285–297.
- [5] Anna Rita Bacinello and Ivan Zoccolan, *Variable annuities with a threshold fee: valuation, numerical implementation and comparative static analysis*, Decisions in Economics and Finance **42** (2019), no. 1, 21–49.
- [6] Bruno Bassan and Claudia Ceci, *Optimal stopping problems with discontinuous reward: Regularity of the value function and viscosity solutions*, Stochastics and Stochastic Reports **72** (2002), no. 1-2, 55–77.
- [7] Daniel Bauer, Jin Gao, Thorsten Moenig, Eric R. Ulm, and Nan Zhu, *Policyholder Exercise Behavior in Life Insurance: The State of Affairs*, North American Actuarial Journal **21** (2017), no. 4, 485–501.
- [8] Daniel Bauer, Alexander Kling, and Jochen Russ, *A Universal Pricing Framework for Guaranteed Minimum Benefits in Variable Annuities*, ASTIN Bulletin: The Journal of the IAA **38** (2008), no. 2, 621–651.
- [9] Carole Bernard, Mary Hardy, and Anne MacKay, *State-Dependent Fees for Variable Annuity Guarantees*, ASTIN Bulletin: The Journal of the IAA **44** (2014), no. 3, 559–585.
- [10] Carole Bernard and Anne MacKay, *Reducing surrender incentives through fee structure in variable annuities*, in: Innovations in Quantitative Risk Management, 2015, pp. 209–223.
- [11] Carole Bernard, Anne MacKay, and Max Muehlbeyer, *Optimal surrender policy for variable annuity guarantees*, Insurance: Mathematics and Economics **55** (2014), 116–128.
- [12] Carole Bernard and Thorsten Moenig, *Where Less Is More: Reducing Variable Annuity Fees to Benefit Policyholder and Insurer*, Journal of Risk and Insurance **86** (2019), no. 3, 761–782.
- [13] Carole Bernard and Junsen Tang, *Variable Annuities with fees tied to VIX*, Working paper, Available at http://egrie2016.ucy.ac.cy/wp-content/uploads/2016/09/16_Bernard_2016-06-13-preliminary.pdf (2016).
- [14] Patrick Billingsley, *Convergence of probability measures*, 2nd ed., John Wiley & Sons, 1999.
- [15] Ning Cai, Steven Kou, and Yingda Song, *A Unified Framework for Regime-Switching Models*, Available at SSRN 3310365 (2019).
- [16] Ning Cai, Yingda Song, and Steven Kou, *A General Framework for Pricing Asian Options Under Markov Processes*, Operations Research **63** (2015), no. 3, 540–554.
- [17] Peter Carr, Robert Jarrow, and Ravi Myneni, *Alternative characterizations of American put options*, Mathematical Finance **2** (1992), no. 2, 87–106.
- [18] Peter Carr and Jian Sun, *A new approach for option pricing under stochastic volatility*, Review of Derivatives Research **10** (2007), 87–150.
- [19] Kyriakos Chourdakis, *Non-Affine Option Pricing*, The Journal of Derivatives **11** (2004), no. 3, 10–25.
- [20] Zhenyu Cui, *Martingale Property and Pricing for Time-Homogeneous Diffusion Models in Finance*, Ph.D. Thesis, 2013.
- [21] Zhenyu Cui, Runhuan Feng, and Anne MacKay, *Variable Annuities with VIX-Linked Fee Structure under a Heston-Type Stochastic Volatility Model*, North American Actuarial Journal **21** (2017), no. 3, 458–483.
- [22] Zhenyu Cui, J. Lars Kirkby, and Duy Nguyen, *Equity-linked annuity pricing with cliquet-style guarantees in regime-switching and stochastic volatility models with jumps*, Insurance: Mathematics and Economics **74** (2017), 46–62.
- [23] ———, *A general framework for discretely sampled realized variance derivatives in stochastic volatility models with jumps*, European Journal of Operational Research **262** (2017), no. 1, 381–400.
- [24] ———, *A General Valuation Framework for SABR and Stochastic Local Volatility Models*, SIAM Journal on Financial Mathematics **9** (2018), no. 2, 520–563.
- [25] ———, *Continuous-Time Markov Chain and Regime Switching Approximations with Applications to Options Pricing*, in: Modeling, Stochastic Control, Optimization, and Applications, 2019, pp. 115–146.
- [26] Zhenyu Cui, Chihoon Lee, and Mingzhe Liu, *Valuation of VIX Derivatives through combined Ito-Taylor Expansion and Markov Chain Approximation*, Working paper of Stevens Institute of Technology, 2021.
- [27] José Da Fonseca and Claude Martini, *The α -hypergeometric stochastic volatility model*, Stochastic Processes and their Applications **126** (2016), no. 5, 1472–1502.
- [28] Tiziano De Angelis and Gabriele Stabile, *On Lipschitz Continuous Optimal Stopping Boundaries*, SIAM Journal on Control and Optimization **57** (2019), no. 1, 402–436.

- [29] Łukasz Delong, *Pricing and hedging of variable annuities with state-dependent fees*, Insurance: Mathematics and Economics **58** (2014), 24–33.
- [30] Kailin Ding and Ning Ning, *Markov chain approximation and measure change for time-inhomogeneous stochastic processes*, Applied Mathematics and Computation **392** (2021), 125732.
- [31] Gabriel G. Drimus, *Options on realized variance by transform methods: a non-affine stochastic volatility model*, Quantitative Finance **12** (2012), no. 11, 1679–1694.
- [32] Stewart N. Ethier and Thomas G. Kurtz, *Markov Processes: Characterization and Convergence*, John Wiley & Sons, 2005.
- [33] Chicago Board Options Exchange, *VIX for Variable Annuities: A study considering the advantages of tying a Variable Annuity fee to VIX*, White Paper (2013(a)), 1–5.
- [34] ———, *VIX for Variable Annuities - Part II: A study considering the advantages of tying a Variable Annuity fee to VIX*, White Paper (2013(b)), 1–16.
- [35] René Garcia, Marc-André Lewis, Sergio Pastorello, and Éric Renault, *Estimation of objective and risk-neutral distributions based on moments of integrated volatility*, Journal of Econometrics **160** (2011), no. 1, 22–32.
- [36] Martino Grasselli, *The $4/2$ stochastic volatility model: A unified approach for the Heston and the $3/2$ model*, Mathematical Finance **27** (2017), no. 4, 1013–1034.
- [37] Geoffrey R. Grimmet and David R. Stirzaker, *Probability and Random Processes*, 3rd edn, Oxford University Press, 2001.
- [38] Anders Grosen and Peter Løchte Jørgensen, *Valuation of Early Exercisable Interest Rate Guarantees*, Journal of Risk and Insurance (1997), 481–503.
- [39] Mary Hardy, *Investment Guarantees: Modeling and Risk Management for Equity-Linked Life Insurance*, John Wiley & Sons, Inc., 2003.
- [40] Steven L. Heston, *A Closed-Form Solution for Options with Stochastic Volatility with Applications to Bond and Currency options*, The Review of Financial Studies **6** (1993), no. 2, 327–343.
- [41] ———, *A Simple New Formula for Options With Stochastic Volatility*, Technical report of Washington University of St. Louis, 1997.
- [42] H. J. Hogben, M. Krzystyniak, G. T. P. Charnock, P. J. Hore, and Ilya Kuprov, *Spinach—A software library for simulation of spin dynamics in large spin systems*, Journal of Magnetic Resonance **208** (2011), no. 2, 179–194.
- [43] John Hull and Alan White, *The Pricing of Options on Assets with Stochastic Volatilities*, The Journal of Finance **42** (1987), no. 2, 281–300.
- [44] Saul D. Jacka, *Optimal stopping and the American put*, Mathematical Finance **1** (1991), no. 2, 1–14.
- [45] Benjamin Jourdain, *Loss of martingality in asset price models with lognormal stochastic volatility*, preprint Cermics **267** (2004), 2004.
- [46] Boda Kang and Jonathan Ziveyi, *Optimal surrender of guaranteed minimum maturity benefits under stochastic volatility and interest rates*, Insurance: Mathematics and Economics **79** (2018), 43–56.
- [47] In Joon Kim, *The Analytic Valuation of American Options*, The Review of Financial Studies **3** (1990), no. 4, 547–572.
- [48] J. Lars Kirkby, Duy Nguyen, and Zhenyu Cui, *A unified approach to bermudan and barrier options under stochastic volatility with jumps*, Journal of Economic Dynamics and Control **80** (2017), 75–100.
- [49] Alexander Kling, Frederik Ruez, and Jochen Ruß, *The impact of policyholder behavior on pricing, hedging, and hedge efficiency of withdrawal benefit guarantees in variable annuities*, European Actuarial Journal **4** (2014), 281–314.
- [50] Michael A. Kouritzin and Anne MacKay, *VIX-linked fees for GMWBs via explicit solution simulation methods*, Insurance: Mathematics and Economics **81** (2018), 1–17.
- [51] Ilya Kuprov, *Diagonalization-free implementation of spin relaxation theory for large spin systems*, Journal of Magnetic Resonance **209** (2011), no. 1, 31–38.
- [52] Harold J. Kushner, *Numerical Methods for Stochastic Control Problems in Continuous Time*, SIAM Journal on Control and Optimization **28** (1990), no. 5, 999–1048.
- [53] Damien Lambertson, *Convergence of the critical price in the approximation of american options*, Mathematical Finance **3** (1993), no. 2, 179–190.
- [54] ———, *American Options*, in: Statistic in Finance, 1998.
- [55] ———, *Brownian Optimal Stopping and Random Walks*, Applied Mathematics & Optimization **45** (2002), 283–324.
- [56] Alvaro Leitao Rodriguez, J. Lars Kirkby, and Luis Ortiz-Gracia, *The CTMC-Heston Model: Calibration and Exotic Option Pricing with SWIFT*, Journal of Computational Finance **24** (2021), no. 4.
- [57] Chia Chun Lo and Konstantinos Skindilias, *An improved Markov chain approximation methodology: Derivatives pricing and model calibration*, International Journal of Theoretical and Applied Finance **17** (2014), no. 7, 1450047.
- [58] Jingtang Ma, Wensheng Yang, and Zhenyu Cui, *CTMC intergral equation method for American options under stochastic local volatility models*, Journal of Economic Dynamics and Control **128** (2021), 104145.
- [59] ———, *Convergence analysis for continuous-time Markov chain approximation of stochastic local volatility models: Option pricing and Greeks*, Journal of Computational and Applied Mathematics **404** (2022), 113901.
- [60] Anne Mackay, *Fee Structure and Surrender Incentives in Variable Annuities*, Ph.D. Thesis, 2014.

- [61] Anne Mackay, Maciej Augustyniak, Carole Bernard, and Mary R Hardy, *Risk Management of Policyholder Behavior in Equity-Linked Life Insurance*, *Journal of Risk and Insurance* **84** (2017), no. 2, 661–690.
- [62] Frederic Mentink-Vigier, *Fast exponential matrix for Matlab (full/sparse), fastExpm*, Available at GitHub (<https://github.com/fmentink/fastExpm/releases/tag/1.0>), Retrieved February 3, 2022.
- [63] Aleksandar Mijatović and Martijn Pistorius, *Continuously monitored barrier options under Markov processes*, Available at SSRN:<https://ssrn.com/abstract=1462822> (2009).
- [64] ———, *Continuously monitored barrier options under Markov processes*, *Mathematical Finance* **23** (2013), no. 1, 1–38.
- [65] Moshe A. Milevsky and Thomas S Salisbury, *The Real Option to Lapse a Variable Annuity: Can Surrender Charges Complete the Market*, Conference Proceedings of the 11th Annual International AFIR Colloquium, 2001.
- [66] Thorsten Moenig and Nan Zhu, *Lapse-and-Reentry in Variable Annuities*, *Journal of Risk and Insurance* **85** (2018), no. 4, 911–938.
- [67] Jari Niittuinperä, *Chapter 18 – Policyholder Behavior and Management Actions*, in: IAA Risk Book, 2020.
- [68] Jan Palczewski and Łukasz Stettner, *Finite Horizon Optimal Stopping of Time-Discontinuous Functionals with Applications to Impulse Control with Delay*, *SIAM Journal on Control and Optimization* **48** (2010), no. 8, 4874–4909.
- [69] Riccardo Rebonato, *Volatility and Correlation: The Perfect Hedger and the Fox*, 2nd edn, John Wiley & Sons, 2004.
- [70] Martin Schweizer, *On Bermudan Options*, in: Advances in Finance and Stochastics, 2002, pp. 257–270.
- [71] Louis O. Scott, *Option Pricing when the Variance Changes Randomly: Theory, Estimation, and an Application*, *Journal of Financial and Quantitative Analysis* **22** (1987), no. 4, 419–438.
- [72] Yang Shen, Michael Sherris, and Jonathan Ziveyi, *Valuation of guaranteed minimum maturity benefits in variable annuities with surrender options*, *Insurance: Mathematics and Economics* **69** (2016), 127–137.
- [73] Roger B. Sidje, *Expokit: a software package for computing matrix exponentials*, *ACM Transactions on Mathematical Software* **24** (1998), no. 1, 130–156.
- [74] Carlos A. Sin, *Complications with stochastic volatility models*, *Advances in Applied Probability* **30** (1998), no. 1, 256–268.
- [75] Qingshuo Song, George Yin, and Qing Zhang, *Weak Convergence Methods for Approximation of the Evaluation of Path-Dependent Functionals*, *SIAM Journal on Control and Optimization* **51** (2013), no. 5, 4189–4210.
- [76] Dominigo Tavella and Curt Randall, *Pricing Financial Instruments: The Finite Difference Method*, John Wiley & Sons (2000).
- [77] Nizar Touzi, *American Options Exercise Boundary When the Volatility Changes Randomly*, *Applied Mathematics and Optimization* **39** (1999), 411–422.
- [78] Gu Wang and Bin Zou, *Optimal fee structure of variable annuities*, *Insurance: Mathematics and Economics* **101, Part B** (2021), 587–601.
- [79] David Williams, *Probability with Martingales*, Cambridge University Press, 1991.
- [80] Gongqiu Zhang and Lingfei Li, *Analysis of Markov Chain Approximation for Option Pricing and Hedging: Grid Design and Convergence Behavior*, *Operations Research* **67** (2019), no. 2, 407–427.
- [81] Yingzi Zhu and Jin E. Zhang, *Variance term structure and VIX futures pricing*, *International Journal of Theoretical and Applied Finance* **10** (2007), no. 1, 111–127.

APPENDIX A. PROOFS OF MAIN RESULTS

A.1. **Proof of Proposition 4.3.** First recall that

$$\begin{aligned}\mathbb{P}(X_{t+h}^{(m,N)} = x_l, V_{t+h}^{(m)} = v_j | X_t^{(m,N)} = x_i, V_t^{(m)} = v_k) \\ = \mathbb{P}(Y_{t+h}^{(m,N)} = (j-1)N + l | Y_t^{(m,N)} = (k-1)N + i).\end{aligned}$$

By inspection of the matrix $\mathbf{G}^{(m,N)}$ and since h is small, we have by (3.1) that

$$\mathbb{P}(X_{t+h}^{(m,N)} = x_l, V_{t+h}^{(m)} = v_j | X_t^{(m,N)} = x_i, V_t^{(m)} = v_k) = \begin{cases} q_{kj}h + c_{ii}^{kj}(h) & \text{if } i = l, j \neq k \\ \lambda_{il}^k h + c_{il}^{kk}(h) & \text{if } i \neq l, j = k \\ 1 + (q_{kk} + \lambda_{ii}^k)h + c_{ii}^{kk}(h) & \text{if } i = l, j = k \\ c_{il}^{kj}(h) & \text{if } i \neq l, k \neq j. \end{cases}$$

where the functions $\{c_{il}^{kj}\}$ satisfy $\lim_{h \rightarrow 0} \frac{c_{il}^{kj}(h)}{h} = 0$ for $i, l \in \{1, 2, \dots, N\}$ and $k, j \in \{1, 2, \dots, m\}$.

From the last equality, we observe that the regime-switching CTMC cannot change regime ($V^{(m)}$) and state ($X^{(m,N)}$) simultaneously over small time intervals.

It follows that

$$\begin{aligned}\mathbb{E} \left[\phi \left(t+h, X_{t+h}^{(m,N)}, V_{t+h}^{(m)} \right) | X_t^{(m,N)} = x_i, V_t^{(m)} = v_k \right] \\ = \sum_{\substack{j=1 \\ j \neq k}}^m \phi(t+h, x_i, v_j) (q_{kj}h + c_{ii}^{kj}(h)) + \sum_{\substack{l=1 \\ l \neq i}}^N \phi(t+h, x_l, v_k) (\lambda_{il}^k h + c_{il}^{kk}(h)) \\ + \phi(t+h, x_i, v_k) (1 + (q_{kk} + \lambda_{ii}^k)h + c_{ii}^{kk}(h)) + \sum_{\substack{j=1 \\ j \neq k}}^m \sum_{\substack{l=1 \\ l \neq i}}^N \phi(t+h, x_l, v_j) c_{il}^{kj}(h) \\ = \phi(t+h, x_i, v_k) + \sum_{j=1}^m \phi(t+h, x_i, v_j) q_{kj}h + \sum_{l=1}^N \phi(t+h, x_l, v_k) \lambda_{il}^k h + c_N(h),\end{aligned}$$

since for $i, l \in \{1, 2, \dots, N\}$ and $j, k \in \{1, 2, \dots, m\}$, $\lim_{h \rightarrow 0} \frac{\phi(t+h, x_l, v_j) c_{il}^{kj}(h)}{h} = 0$.

Also observe that

$$\begin{aligned}\mathbb{E} \left[\phi(t+h, X_{t+h}^{(m,N)}, v_j) | V_t^{(m)} = V_{t+h}^{(m)} = v_j, X_t^{(m,N)} = x_i \right] \\ = \sum_{l=1}^N \phi(t+h, x_l, v_j) \mathbb{P} \left(X_{t+h}^{(m,N)} = x_l | V_t^{(m)} = V_{t+h}^{(m)} = v_j, X_t^{(m,N)} = x_i \right) \\ = \sum_{\substack{l=1 \\ l \neq i}}^N \phi(t+h, x_l, v_j) (\lambda_{il}^j h + c_{il}^j(h)) + \phi(t+h, x_i, v_j) (1 + \lambda_{ii}^j h + c_{ii}^j(h)) \\ = \phi(t+h, x_i, v_j) + \sum_{l=1}^N \phi(t+h, x_l, v_j) (\lambda_{il}^j h + c_{il}^j(h)).\end{aligned}$$

Hence, we have that

$$\begin{aligned}\sum_{j=1}^m \mathbb{E} \left[\phi(t+h, X_{t+h}^{(m,N)}, v_j) | V_t^{(m)} = V_{t+h}^{(m)} = v_j, X_t^{(m,N)} = x_i \right] \mathbb{P} \left(V_{t+h}^{(m)} = v_j | V_t^{(m)} = v_k \right) \\ = \sum_{j=1}^m \left(\phi(t+h, x_i, v_j) + \sum_{l=1}^N \phi(t+h, x_l, v_j) (\lambda_{il}^j h + c_{il}^j(h)) \right) (q_{kj}h + c_{kj}(h))\end{aligned}$$

$$\begin{aligned}
& + \phi(t+h, x_i, v_k) + \sum_{l=1}^N \phi(t+h, x_l, v_k) (\lambda_{il}^k h + c_{il}^k(h)) \\
= & \phi(t+h, x_i, v_k) + \sum_{j=1}^m \phi(t+h, x_i, v_j) q_{kj} h + \sum_{l=1}^N \phi(t+h, x_l, v_k) \lambda_{il}^k h + c_m(h).
\end{aligned}$$

where the second line follows from

$$\mathbb{P}\left(V_{t+h}^{(m)} = v_j \mid V_t^{(m)} = v_k\right) = \begin{cases} 1 + q_{kk}h + c_{kk}(h) & \text{if } j = k \\ q_{kj}h + c_{kj}(h) & \text{if } j \neq k. \end{cases}$$

The results follows from setting $c(h) = c_m(h) - c_N(h)$. ■

A.2. Proof of Proposition 4.5. In order to prove Proposition 4.5, we first need to introduce some additional notation.

Suppose that $t = 0$. For $0 \leq s \leq T$, define the discounted reward process of the original contract by

$$Z_s = e^{-rs} \varphi(s, F_s, V_s),$$

and the discounted reward process of the modified contract with M possible exercise dates by

$$\tilde{Z}_s^{(M)} = Z_s \mathbf{1}_{\{s \in \mathcal{H}_M\}}.$$

Let the process $\{J_t^{(M)}\}_{0 \leq t \leq T}$ be defined by

$$(A.1) \quad J_t^{(M)} = \operatorname{ess\,sup}_{\tau \in \mathcal{T}_{\Delta, M}, \tau \geq t} \mathbb{E}_t[Z_\tau],$$

and the process $\{\tilde{J}_t^{(M)}\}_{0 \leq t \leq T}$ be defined by

$$(A.2) \quad \tilde{J}_t^{(M)} = \operatorname{ess\,sup}_{\tau \in \mathcal{T}, \tau \geq t} \mathbb{E}_t[\tilde{Z}_\tau^{(M)}].$$

As explained in [70], since the Bermudan contract cannot be exercised outside the region of permitted exercise times and Z is non-negative, we expect the value of the Bermudan contract with the payoff process Z to be equivalent to an American contract with the payoff process $\tilde{Z}^{(M)}$. That is, we expect $J^{(M)}$ to be equal to $\tilde{J}^{(M)}$, almost surely. This idea is formalized in [70], Proposition 3 which is restated in the following lemma.

Lemma A.1 ([70], Proposition 3). *Fix $M \in \mathbb{N}$ and let $J^{(M)}$ and $\tilde{J}^{(M)}$ be defined as in (A.1) and (A.2), respectively, then $J^{(M)} = \tilde{J}^{(M)}$, almost surely.*

We can now prove Proposition 4.5.

Proof of Proposition 4.5. The following is inspired by the proof of Proposition 6 of [6].

Without loss of generality, suppose that $t = 0$. We showed in Lemma A.1 that $J_t^{(M)} = \tilde{J}_t^{(M)}$, almost surely. Hence, the Bermudan contract in (4.6) may be expressed as follows:

$$b_M(0, x, y) = \sup_{\tau \in \mathcal{T}_{0, T}} \mathbb{E}_{x, y}[\tilde{Z}_\tau^{(M)}],$$

Now notice that for each t , $\{\tilde{Z}_t^{(M)}\}_{M \in \mathbb{N}}$ is an increasing sequence of random variables converging to Z_t pointwisely, that is, for each $t \geq 0$, $\tilde{Z}_t^{(M)}(\omega) \uparrow Z_t(\omega)$ for all $\omega \in \Omega$. Thus, given $F_0 = x$ and $V_0 = y$ and by using the monotone convergence theorem ([79], Theorem 5.3), we obtain

$$\begin{aligned}
v(0, x, y) &= \sup_{\tau \in \mathcal{T}_{0, T}} \mathbb{E}[Z_\tau] = \sup_{\tau \in \mathcal{T}_{0, T}} \mathbb{E}[\sup_{M \in \mathbb{N}} \tilde{Z}_\tau^{(M)}] = \sup_{\tau \in \mathcal{T}_{0, T}} \sup_{M \in \mathbb{N}} \mathbb{E}[\tilde{Z}_\tau^{(M)}] \\
&= \sup_{M \in \mathbb{N}} \sup_{\tau \in \mathcal{T}_{0, T}} \mathbb{E}[\tilde{Z}_\tau^{(M)}] = \sup_{M \in \mathbb{N}} b_M(0, x, y) = \lim_{M \rightarrow \infty} b_M(0, x, y).
\end{aligned}$$
■

APPENDIX B. SUPPLEMENTAL MATERIAL

This document provides supplemental material to Analysis of VIX-Linked Fee Incentives in Variable Annuities via Continuous-Time Markov Chain Approximation.

B.1. Accuracy of the VA price and the Approximated Optimal Surrender Strategy.

The purpose of this subsection is to analyze numerically the accuracy of Algorithm 4 to approximate the optimal surrender strategy. In the context of American put options under the Black-Scholes setting, [53] considers a similar approximation for the exercise boundary when the underlying diffusion process is approximated by a Markov chain. In particular, under this setting, [53] proves theoretically the convergence of the approximated exercise boundary (also called the critical price) towards the exact exercise boundary in their Theorem 2.1.

In order to analyze the accuracy of our methodology against a known benchmark, we use our algorithms in a problem that has been done by others. More precisely, we compare the approach of Algorithm 4 (also called the CTMC Bermudian approximation and denoted below by “CTMC-Berm”) for approximating the optimal surrender surface and the value of a variable annuity with early surrenders to the ones obtained using the approach of [11], the “Benchmark”. The methodology proposed by [11] is based on the integral equation method of [47] under the Black-Scholes model, and cannot be easily extended to more general models. Thus, in order to compare with their method, we assume that the volatility of the index is constant so that

$$dS_t = rS_t dt + \sigma S_t dW_t, \quad t \geq 0,$$

where $\sigma > 0$ is the volatility. We also suppose that $c(x, y) = \tilde{c} > 0$, for all $(x, y) \in \mathbb{R}_+ \times \mathcal{S}_V$, and we use $g(t, y) = 1$ for all $(t, y) \in [0, T] \times \mathcal{S}_V$. Hence, the VA account dynamics is given by

$$dF_t = (r - \tilde{c})F_t dt + \sigma F_t dW_t, \quad 0 \leq t \leq T.$$

We approximate the logarithm of the fund process $\tilde{X}_t = \ln F_t$, $0 \leq t \leq T$ by using CTMC approximation method. The CTMC approach for one-dimensional diffusion processes works in the exact same way as the one described in Subsection 3.1 for the approximation of V , see [25] for details. The number of state-space grids and time steps are set to $N = 5,000$ and $M = T \times 500$, respectively. We use the grid of [76], as discussed in Section 5.1, with a non-uniformity parameter $\tilde{\alpha}_{\tilde{X}} = 5$. The grid upper (\tilde{x}_N) and lower bounds (\tilde{x}_1) of the approximated process \tilde{X} are set about the mean of \tilde{X}_t at $t = T/2$ as follows: $\tilde{x}_N = \bar{\mu}(t) + \gamma\bar{\sigma}(t)$ and $\tilde{x}_1 = \bar{\mu}(t) - \gamma\bar{\sigma}(t)$ where $\bar{\mu}(t)$ is the conditional mean of \tilde{X}_t given \tilde{X}_0 and $\bar{\sigma}(t)$, the conditional standard deviation. We use $\gamma = 7.2$. Now note that, under the Black-Scholes setting, we have

$$\bar{\mu}(t) = \tilde{X}_0 + \left(r - \frac{\sigma^2}{2}\right)t, \quad \text{and} \quad \bar{\sigma}(t) = \sigma\sqrt{t}.$$

As a benchmark, we use the value of the variable annuity with early surrenders and the optimal surrender boundary obtained using the method of [11] with 1500 steps per year. Other parameters are $G = 100$, $r = 0.03$ and $T = 15$. We tested our method for different volatility levels $\sigma \in \{0.1, 0.2, 0.3, 0.4\}$ and initial values of the VA account $F_0 \in \{90, 100\}$. The fair fee \tilde{c}^* is calculated such that the expected discounted value of the maturity benefit equals the value of the VA account at inception, that is $F_0 = \mathbb{E}[e^{-rT} \max(G, F_T)]$. We compare to the benchmark the value of the variable annuity with early surrenders “VA with ES” and the optimal surrender boundary (“Opt. Surre. Bound.”). The results are reported in Table 8. The column “Rel. Err.” documents the relative errors whereas “Max Re. Err” documents the maximum relative errors²⁰.

From Table 8, we see that the CTMC Bermudian approximation achieves a high level of accuracy across all volatility levels and initial value of VA account F_0 .

²⁰Given a benchmark value y and its approximation y_{approx} , the relative error is defined as $|y - y_{approx}|/|y|$ for $y \neq 0$; whereas the maximum relative error is the largest relative error over a sample of benchmark values and their approximations.

	σ	\tilde{c}^* (%)	VA with ES			Opt. Surre. Bound.
			CTMC-Berm	Bernard et al. (2014)	Rel. Err.	Max Rel. Err.
$F_0 = 100$	0.1	0.1374	100.851600	100.851748	1.47e-6	2.60e-3
	0.2	0.9094	104.400379	100.401287	8.70e-6	5.20e-3
	0.3	1.9277	108.577366	108.579001	1.51e-5	7.78e-3
	0.4	2.9415	112.823616	112.826112	2.21e-5	1.04e-2
$F_0 = 90$	0.1	0.2641	91.28494	91.285171	2.53e-6	2.60e-3
	0.2	1.3062	94.989758	94.990712	1.01e-5	5.20e-3
	0.3	2.5571	99.012022	99.013806	1.80e-5	7.78e-3
	0.4	3.7631	103.022547	103.025197	2.57e-5	1.03e-2

TABLE 8. Relative errors of a variable annuities with ES and maximum relative errors of the optimal surrender boundaries.

B.2. Accuracy and efficiency of the CTMC approximation for the VIX index. We assess the accuracy of the CTMC approximation for the volatility index for the 3/2 and Heston models. Under a Heston-type model, the VIX has a closed-form expression given by

$$(B.1) \quad \text{VIX}_t^2 = B + AV_t$$

with $A = \frac{1-e^{-\kappa\tau}}{\kappa\tau}$ and $B = \frac{\theta(\kappa\tau-1+e^{-\kappa\tau})}{\kappa\tau}$, see [81] for details.

For the 3/2 model, a closed-form expression for the VIX may be found in [18], Theorem 4. However, as pointed out by [31], the integral that appears in the analytical formula is difficult to implement and is not suited for fast and accurate numerical approximation. For this reason, benchmark results are obtained via Monte Carlo simulation²¹ under 3/2 model.

The market and CTMC parameters are set to the ones of Subsection 5.1 for the Heston model, except that we set $m = 1,000$ (rather than $m = 50$). For the 3/2 model, we use the parameters reported in Section B.5.1. The results are presented in Table 9. The column “ V_t ” (resp. $1/V_t$) displays the initial value of the variance at time $t \geq 0$ for the Heston model (resp. the 3/2 model), the column “CTMC” shows the result of the VIX approximation using Algorithm 6 with $n = 1,000$ time steps, and the column “Benchmark” reports the benchmark value calculated either by using the closed-form formula (B.1) (for the Heston model) or by Monte Carlo simulation (for the 3/2 model). The relative error are documented in column “Rel. err”.

V_t	CTMC	Benchmark	Rel. err.	$1/V_t$	CTMC	Benchmark	Rel. err.
0.01	11.1077%	11.1068%	8.10e-05	0.01	11.2202%	11.2203%	8.91e-06
0.02	14.6829%	14.6824%	3.41e-05	0.02	15.7016%	15.7020%	2.55e-05
0.04	20.0000%	20.0000%	0.00e+00	0.04	21.4892%	21.4901%	4.19e-05
0.06	24.1746%	24.1749%	1.24e-05	0.06	25.3096%	25.3112%	6.32e-05
0.09	29.3433%	29.3439%	2.04e-05	0.09	29.2708%	29.2735%	9.22e-05

(A) Heston model

(B) 3/2 model

TABLE 9. Accuracy of the CTMC- VIX approximation, Algorithm 6

The results of Table 9 confirm the high accuracy of the CTMC-VIX approximation for both models. It is worth mentioning that, when using Algorithm 6, we obtain simultaneously the value of the $\text{VIX}_t^{(m),k}$ for all $v_k \in \mathcal{S}_V^{(m)}$ within less than a 0.1 second for both models. The value of the

²¹We simulate 500K paths (plus 500K antithetic variables) using Milstein discretization scheme and we use 5,000 time steps.

CTMC approximation given a particular value for V_t is then interpolated between the appropriate grid points. This further increases the efficiency of our algorithm.

B.3. VA prices accuracy and computation time under the Heston model. Table 10 shows the value of a variable annuity with and without surrender rights (“VA with ES” and “VA without ES”, respectively) under the Heston model with the Uncapped VIX²-linked fees using $N = 100$, $N = 1,100$ and $M = 252 \times 10$; and using $N = 2,000$ and $M = 500 \times 10$. All other market, VA and CTMC parameters are the same as in Subsection 5.1.

	$\tilde{m}^* =$ $c^* =$	0.0000	0.1500	0.3000	0.4345	
		1.5338%	1.0036%	0.4741%	0.000%	Computation Time (sec.)
VA without ES	$N = 2,000$	100.00090	100.00091	100.00092	100.00093	2,500
	$N = 1,100$	100.00094	100.00095	100.00096	100.00097	400
	$N = 100$	100.00750	100.00769	100.00789	100.00807	0.85
VA with ES	$N = 2,000$	103.01785	103.00823	103.00330	103.00367	7,100
	$N = 1,100$	103.01743	103.00788	103.00300	103.00341	1,600
	$N = 100$	103.0162	103.00676	103.00190	103.00228	54
ES value	$N = 2,000$	3.01695	3.00732	3.00238	3.00274	N/A
	$N = 1,100$	3.01649	3.00693	3.00204	3.00243	N/A
	$N = 100$	3.00862	2.99907	2.99401	2.99421	N/A

TABLE 10. Variable annuity with and without early surrenders using CTMC Approximation with $N = 100$ and $1,100$, with $M = 252 \times 10$; and $N = 2,000$ with $M = 500 \times 10$.

All the numerical results and computation times in Table 10 are performed using Equation 4.2 and Algorithm 2 combine with the Expokit procedures of [73], function *expv*. Since fair fees are calibrated at inception using the exact pricing formula of [21], the benchmark value for the VA without surrender rights is $F_0 = 100$. When $N = 100$, accurate VA prices are obtained extremely fast (within 54 sec. for the VA with surrender rights and less than a second for the VA without surrender rights). The absolute error is around 10^{-3} for both values²².

Similar results are obtained with the Fast Algorithms (1, 3 and 5). The results are reported in Table 11. The values of VA with and without surrender rights are calculated simultaneously, as per Remark 5.2. So, the computation times in column “Computation Time (sec.)” are for both prices.

	$\tilde{m}^* =$ $c^* =$	0.0000	0.1500	0.3000	0.4345	
		1.5338%	1.0036%	0.4741%	0.000%	Computation Time (sec.)
VA without ES	$N = 2,000$	99.99615	99.99611	99.99607	99.99603	N/A
	$N = 1,100$	99.99619	99.99615	99.99611	99.99607	N/A
	$N = 100$	100.00276	100.00290	100.00304	100.00317	N/A
VA with ES	$N = 2,000$	103.02361	103.01360	103.00815	103.00789	4,405
	$N = 1,100$	103.02360	103.01359	103.00814	103.00788	1,244
	$N = 100$	103.02237	103.01251	103.00715	103.00680	9.60
ES value	$N = 2,000$	3.02745	3.01748	3.01208	3.01186	N/A
	$N = 1,100$	3.02741	3.01744	3.01203	3.01181	N/A
	$N = 100$	3.01961	3.00961	3.00411	3.00363	N/A

TABLE 11. Variable annuity with and without early surrenders (ES) using CTMC Approximation Fast Algorithms with $N = 100$ and $1,100$, with $M = 500 \times 10$; and $N = 2,000$ with $M = 500 \times 10$.

²²The benchmark for the VA with early surrenders is the approximated CTMC value obtained using $N = 2,000$ and $M = 500$.

By comparing the two tables, we note that the Fast Algorithms provide very accurate results extremely fast²³ compared to the original Algorithms

B.4. Other Numerical Analysis of VIX-linked Fee Incentives in the Heston Model. In this appendix, we show the numerical results obtained under the Heston model for the three fee structures (Uncapped VIX², Capped VIX² and Uncapped VIX), detailed in Subsection 5.3, when the guaranteed amount is set to $G = F_0 e^{\tilde{g}T}$ with $\tilde{g} = 2\%$ (rather than $G = F_0$). The conclusions are similar to the ones detailed in Subsection 5.4.

Unless stated otherwise, in this section, all market, VA and CTMC parameters are the same as in Subsection 5.1. except for $G = F_0 e^{\tilde{g}T}$ with $\tilde{g} = 2\%$ and $M = T \times 252$.

Fair fee parameters $(\tilde{c}^*, \tilde{m}^*)$ are presented in Table 12a, whereas Table 12b shows the approximated values of early surrenders. When $c_t = \tilde{c}^* + \tilde{m}^* \text{VIX}_t^2$, the fair parameters are obtained using the exact formula of [21]. For the other fee structures, the fair parameters are obtained using CTMC approximation with $N = 100$, $m = 50$ and $M = T \times 252$ to accelerate the computation time.

	$c_t = \tilde{c}^* + \tilde{m}^* \text{VIX}_t^2$					$c_t = \tilde{c}^* + \tilde{m}^* \text{VIX}_t^2$			
\tilde{m}^*	0.0000	0.3000	0.8000	1.1313	\tilde{m}^*	0.0000	0.3000	0.8000	1.1313
\tilde{c}^*	3.82542%	2.80632%	1.11545%	0.0000%	ES Value	5.00216	5.01219	5.03998	5.06681
	$c_t = \min\{\tilde{c}^* + \tilde{m}^* \text{VIX}_t^2, K\}, K = 4.5\%$					$c_t = \min\{\tilde{c}^* + \tilde{m}^* \text{VIX}_t^2, K\}, K = 4.5\%$			
\tilde{m}^*	0.0000	0.3000	0.8000	1.4144	\tilde{m}^*	0.0000	0.3000	0.8000	1.4144
\tilde{c}^*	3.82542%	2.83600%	1.45530%	0.0000%	ES Value	5.00216	5.00415	4.98201	4.95968
	$c_t = \tilde{c}^* + \tilde{m}^* \text{VIX}_t$					$c_t = \tilde{c}^* + \tilde{m}^* \text{VIX}_t$			
\tilde{m}^*	0.0000	0.0750	0.1250	0.2128	\tilde{m}^*	0.0000	0.0750	0.1250	0.2128
\tilde{c}^*	3.82542%	2.47570%	1.57660%	0.00000%	ES Value	5.00216	5.00351	5.00569	5.01254
	(A) Fair fee vectors $(\tilde{c}^*, \tilde{m}^*)$					(B) Early surrender values ("ES" values).			

TABLE 12. Fair fee vectors and approximated early surrender values under Heston model when $G = F_0 e^{\tilde{g}T}$, $\tilde{g} = 2\%$

Figures 5, 6 and 7 display the approximated optimal surrender surfaces under the Heston model for the three fee structures when $G = F_0 e^{\tilde{g}T}$ with $\tilde{g} = 2\%$.

²³Recall that the computation times in Table 11 for the Fast Algorithms are for the value of the VAs with and without ES simultaneously.

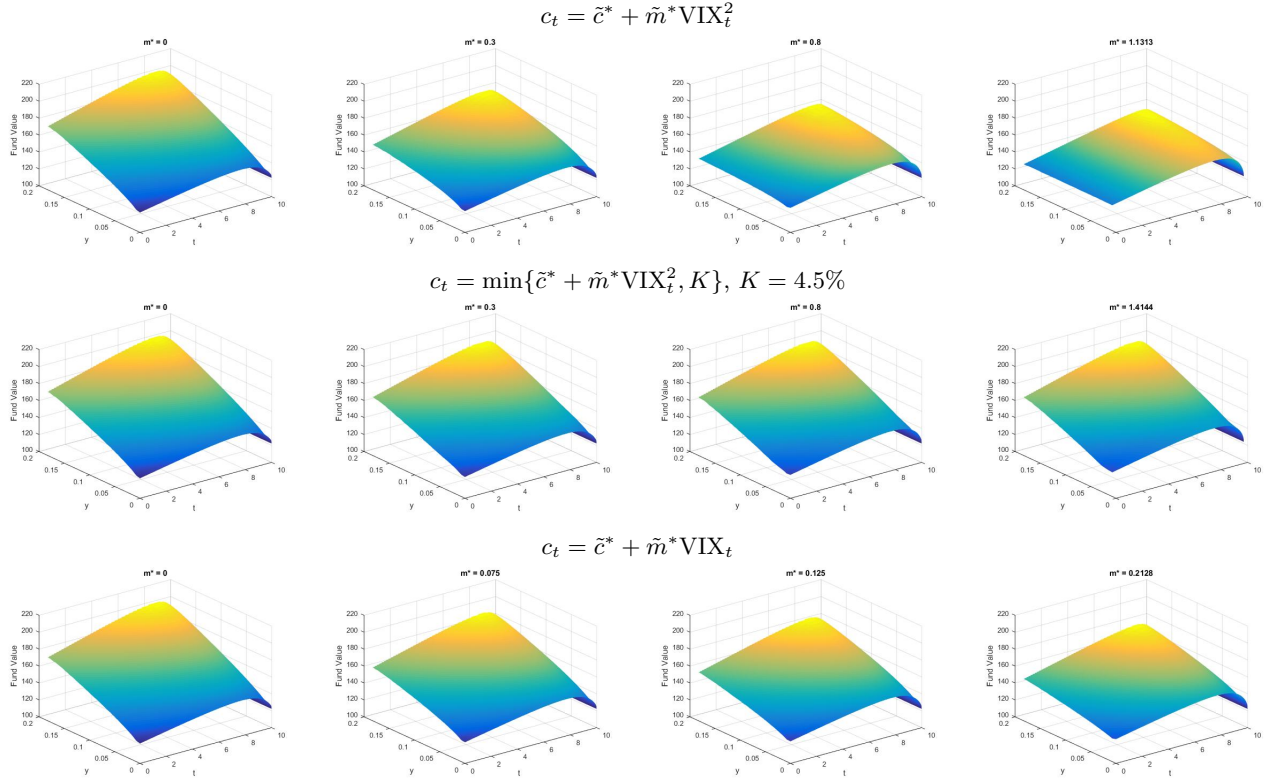


FIGURE 5. Approximated optimal surrender surfaces for different values of fair multiplier \tilde{m}^* under the Heston model, $G = F_0 e^{\tilde{g}T}$ with $\tilde{g} = 2\%$.

B.5. Numerical Analysis under 3/2 Model. In this section, we analyse numerically the impact of VIX-linked fee incentives under the 3/2 model.

B.5.1. Market, VA and CTMC Parameters. In order for the results under the 3/2 model to be comparable to the ones obtained under the Heston model, the market parameters (θ , κ and σ for the 3/2 model) are calibrated to at-the-money call options²⁴ priced using the Heston model with the market parameters in Table 2. The initial value of the variance is set to $V_0 = 0.03$ for the Heston model and $V_0 = 1/0.03$ for the 3/2 model. The correlation $\rho = -0.75$ and the risk-free rate $r = 0.03$ are assumed to be the same under both models. The resulting market parameters are presented in Table 13 and the model dynamics is given in Table 1

Parameter	V_0	κ	θ	σ	ρ	r
Value	1/0.03	5.7488	46.1326	15.4320	-0.75	0.03

TABLE 13. Market parameters for 3/2 model

Unless stated otherwise, all numerical experiments in this section are performed using the CTMC parameters listed in Table 14. Note that for the 3/2 model, the VIX is approximated using Algorithm 6 with $n = 1,000$ time steps, whereas in the Heston model, the volatility index is calculated using a closed-form formula.

²⁴We consider 4 options with maturity $T = 0.5, 2.5, 5$ and 10 . We used $S_0 = K = 100$ and a dividend yield of 1.5338% .

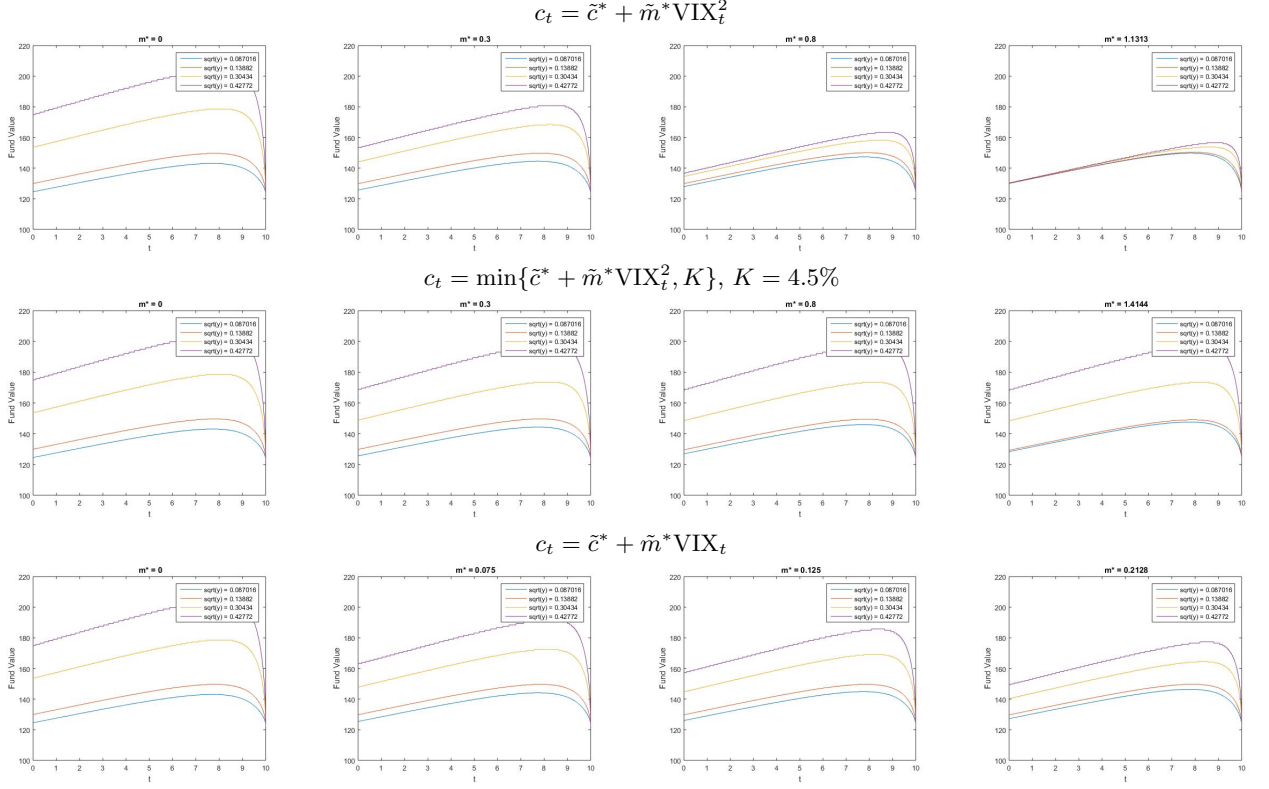


FIGURE 6. The y section of the approximated optimal surrender surface under the Heston model, $f_y^{(m,N)}$, for different volatility levels \sqrt{y} and fair multipliers \tilde{m}^* , $G = F_0 e^{\tilde{g}T}$ with $\tilde{g} = 2\%$.

Parameter	m	N	v_1	v_m	$\tilde{\alpha}_v$	x_1	x_N	$\tilde{\alpha}_X$	M	n
Value	1,000	1,000	$V_0/200$	$8v_0$	0.5764	$-X_0$	$2X_0$	$2/100$	5,000	1,000

TABLE 14. CTMC Parameters for 3/2 Model

B.5.2. *Fee Structures and Fair Fee Parameters.* As for the Heston model, we consider three fee structures: the Uncapped VIX², the Capped VIX² and the Uncapped VIX, see Section 5.3 for details. The fair parameters are calibrated using a CTMC approximation with $N = 100$ (all other CTMC parameters are the same as in Table 14), to reduce the computation time. Table 15 presents the fair fee vectors $(\tilde{c}^*, \tilde{m}^*)$ obtained under the 3/2 model. Note how close the fair fee vectors obtained under the 3/2 model (Table 15) are from the ones obtained under the Heston model (Table 4).

B.5.3. *Effect of VIX-Linked Fees on Surrender Incentives.* Recall from Table 1 that under the 3/2 model, the dynamics of the index and the variance processes are given by²⁵

$$(B.2) \quad \begin{aligned} dS_t &= rS_t dt + \frac{1}{\sqrt{V_t}} S_t dW_t^{(1)}, \\ dV_t &= \kappa(\theta - V_t) dt + \sigma\sqrt{V_t} dW_t^{(2)}, \end{aligned}$$

²⁵Note that in this formulation of the 3/2 model, the process V represents the inverse of the variance process. It is also common to see the 3/2 model expressed in terms of its variance, see for instance [31].

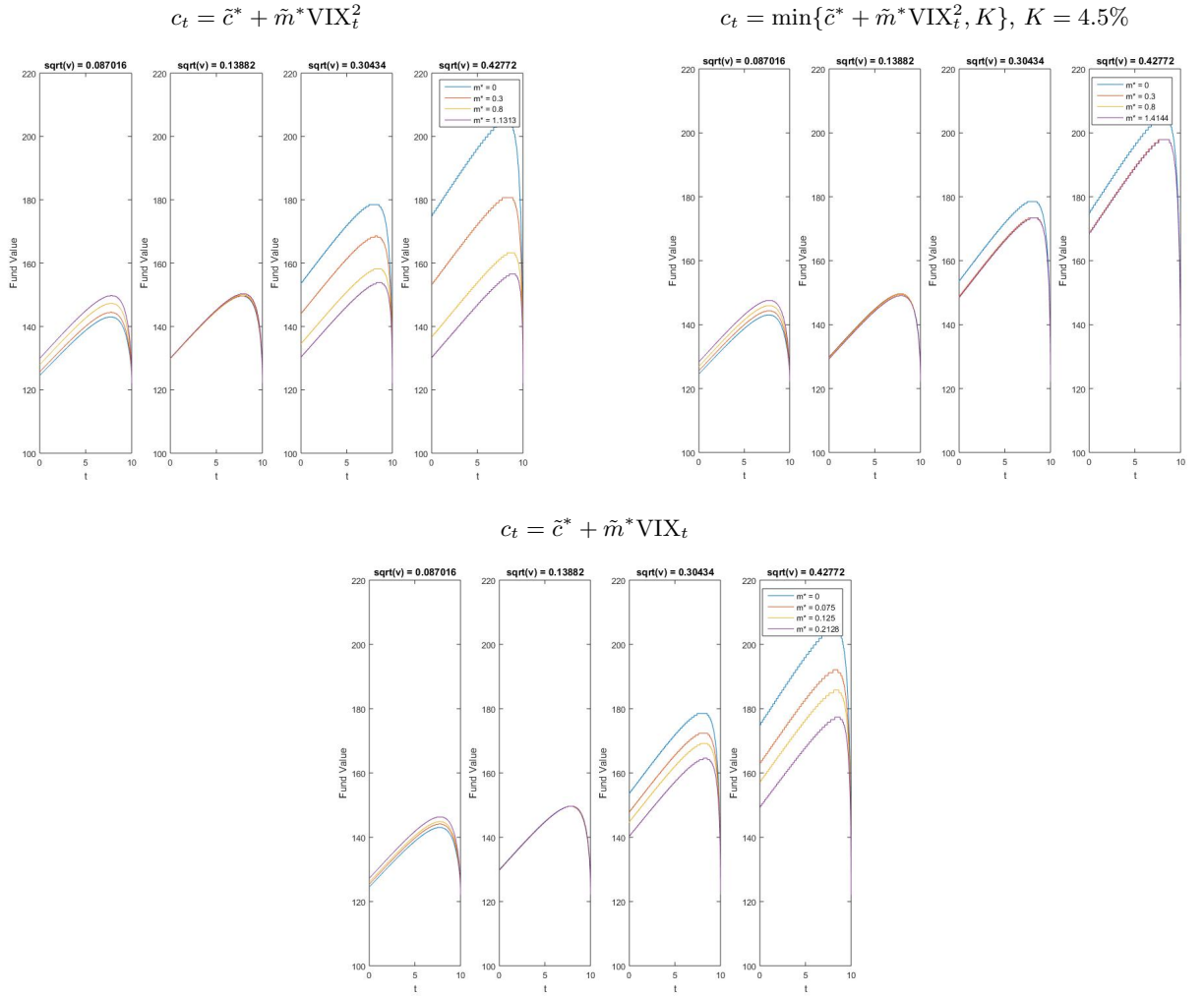


FIGURE 7. The y section of the approximated optimal surrender surface under the Heston model, $f_y^{(m,N)}$, for different volatility levels \sqrt{y} and fair multipliers \tilde{m}^* , $G = F_0 e^{\tilde{g}T}$ with $\tilde{g} = 2\%$.

	$c_t = \tilde{c}^* + \tilde{m}^* \text{VIX}_t^2$			
\tilde{m}^*	0.0000	0.15000	0.3000	0.4235
\tilde{c}^*	1.5273%	0.9858%	0.4449%	0.0000%
	$c_t = \min\{\tilde{c}^* + \tilde{m}^* \text{VIX}_t^2, K\}, K = 2\%$			
\tilde{m}^*	0.0000	0.1500	0.3000	0.5791
\tilde{c}^*	1.5273%	1.0335%	0.6351%	0.0000%
	$c_t = \tilde{c}^* + \tilde{m}^* \text{VIX}_t$			
\tilde{m}^*	0.0000	0.0250	0.0500	0.0846
\tilde{c}^*	1.5273%	1.0757%	0.6241%	0.0000%

TABLE 15. Fair fee vectors $(\tilde{c}^*, \tilde{m}^*)$ under 3/2 model

where $W = (W^{(1)}, W^{(2)})^T$ is a bi-dimensional correlated Brownian motion under \mathbb{Q} and such that $[W^{(1)}, W^{(2)}]_t = \rho t$ with $\rho \in [-1, 0]$ ²⁶, and $\kappa, \theta, \sigma > 0$ with $2\kappa\theta > \sigma^2$.

²⁶The parameter ρ is assumed to be non-positive for the martingale measure to exist, see Footnote 6 for details.

Now from Lemma 3.3, we find that $\gamma(x) = \frac{\ln(x)\rho}{\sigma}$. Thus, given a certain fee process $\{c_t\}_{0 \leq t \leq T}$ (see Subsection 5.3 for examples), the dynamics of the auxiliary process is obtained as follows

$$(B.3) \quad \begin{aligned} dX_t &= \mu_X(X_t, Y_t) dt + \sigma_X(Y_t) dW_t^*, \\ dV_t &= \mu_V(V_t) dt + \sigma_V(V_t) dW_t^{(2)}, \end{aligned}$$

where $\mu_X(X_t, V_t) = r - c_t + \frac{\rho\kappa}{\theta} + \frac{1}{V_t} \left(\frac{\rho\sigma}{2} - \frac{1}{2} - \frac{\rho\kappa\theta}{\sigma} \right)$, and $\sigma_X(V_t) = \sqrt{\frac{1-\rho^2}{V_t}}$, $0 \leq t \leq T$.

When the fee is tied to the VIX, the form of the fee function is not known explicitly at this point under the 3/2 model, since the the VIX does not have a closed-form expression (see footnote 14 for details). However, as illustrated in (3.11), when the inverse variance process V is replaced by its CTMC approximation $V^{(m)}$, the auxiliary process X becomes a RS diffusion $X^{(m)}$ with the following dynamics:

$$(B.4) \quad dX_t^{(m)} = r - c_t^{(m)} + \frac{\rho\kappa}{\theta} + \frac{1}{V_t^{(m)}} \left(\frac{\rho\sigma}{2} - \frac{1}{2} - \frac{\rho\kappa\theta}{\sigma} \right) dt + \sigma_X(V_t^{(m)}) dW_t^*, \quad t \geq 0,$$

where $c_t^{(m)} = c(X_t^{(m)}, V_t^{(m)})$ is the CTMC approximation of the fee process.

Recall that $VIX^{(m)}$ is the CTMC approximation of the volatility index, see Proposition 4.13 and Algorithm 6. The three fee structures exposed in Subsection 5.3 can then be approximated using $VIX^{(m)}$ as shown in Table 16.

Fee Structure	$c_t^{(m)}, 0 \leq t \leq T$
Uncapped VIX ²	$c_t^{(m)} = \tilde{c} + \tilde{m}(VIX_t^{(m)})^2$
Capped VIX ²	$c_t^{(m)} = \min\{K, \tilde{c} + \tilde{m}(VIX_t^{(m)})^2\}$
Uncapped VIX	$c_t^{(m)} = \tilde{c} + \tilde{m}VIX_t^{(m)}$

TABLE 16. CTMC approximation of the VIX-linked fee process

The second layer CTMC approximation of Subsection 3.2 is then applied to the regime-switching diffusion (B.4) with the approximated fee processes listed in Table 16.

Using the CTMC technique outlined in Section 3; and the market, the variable annuity, and the CTMC parameters of Subsection B.5.1, we performed the valuation of a variable annuity with and without early surrenders. The results are similar to the ones obtained under the Heston model and are summarized below, confirming again that fees tied to the volatility index do not significantly affect the value of surrender incentives.

The value of early surrenders (“ES values”) under the 3/2 model are presented in Table 17. The approximated optimal surrender surfaces for the three fee structures under the 3/2 model are displayed in Figures 8, 9 and 10. Note that in order for the Figures under the Heston and 3/2 models to be comparable, the y -axis under the 3/2 model represents the variance of the fund, that is $\frac{1}{V_t}$, $0 \leq t \leq T$ (recall that V is the inverse variance in (B.2)). As noted previously, we observe that the optimal surrender surface is increasing with the volatility. However, when $\tilde{m}^* = 0$, the surrender surface increases much faster than under the Heston model. We also note that VIX-linked fees help to neutralize the effect of the volatility on the optimal surrender decision, confirming again the relation existing between the fees and the optimal surrender strategies; that is, VA contracts with high fees are surrendered at lower fund values than VA contracts with low fees.

$c_t = \tilde{c}^* + \tilde{m}^* \text{VIX}_t^2$				
\tilde{m}^*	0.0000	0.1500	0.3000	0.4235
ES Value	2.91799	2.91126	2.90875	2.91078
$c_t = \min\{\tilde{c}^* + \tilde{m}^* \text{VIX}_t^2, K\}, K = 2\%$				
\tilde{m}^*	0.0000	0.1500	0.3000	0.5791
ES Value	2.91799	2.90594	2.89435	2.88076
$c_t = \tilde{c}^* + \tilde{m}^* \text{VIX}_t$				
\tilde{m}^*	0.0000	0.0250	0.0500	0.0846
ES Value	2.9180	2.9120	2.9068	2.9012

TABLE 17. Approximated early surrender values (ES values) under the 3/2 model.

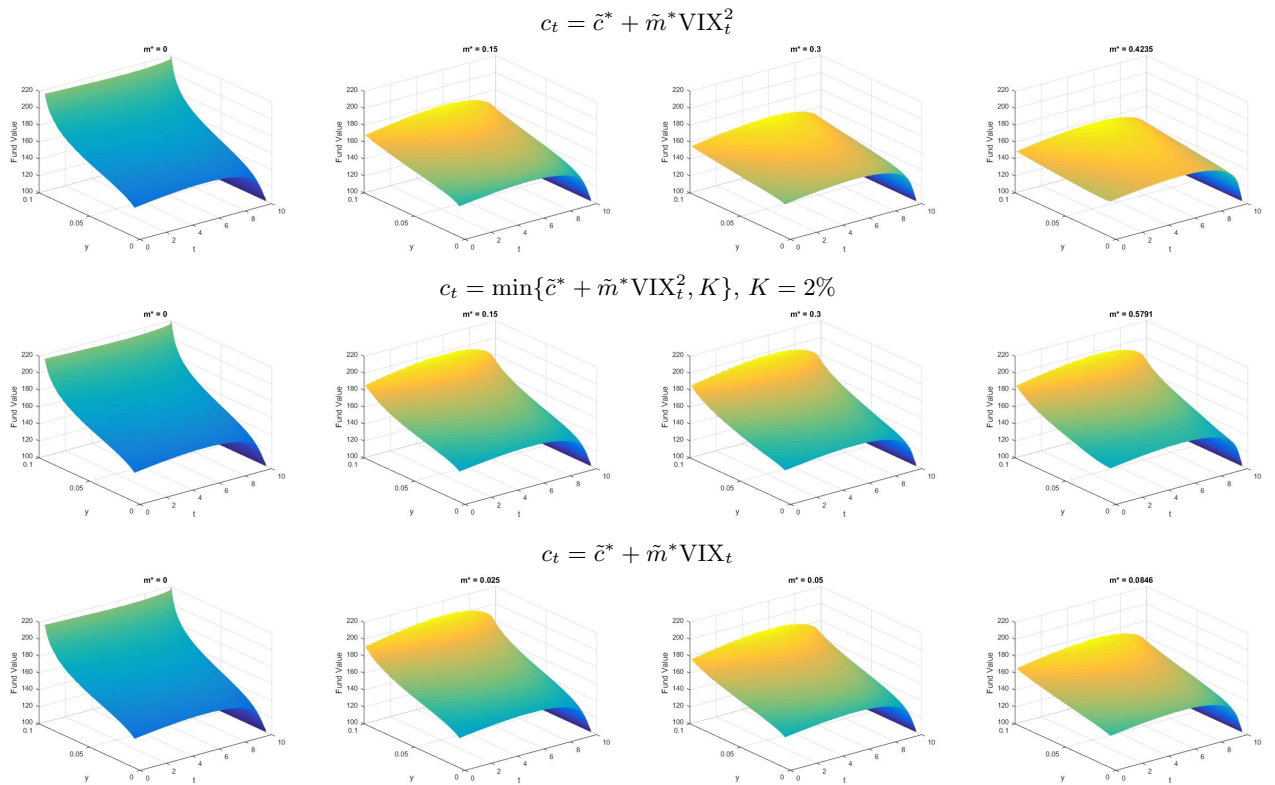


FIGURE 8. Approximated optimal surrender surface for different values of fair multiplier \tilde{m}^* under the 3/2 model where x -axis represents the time and the y -axis the variance.

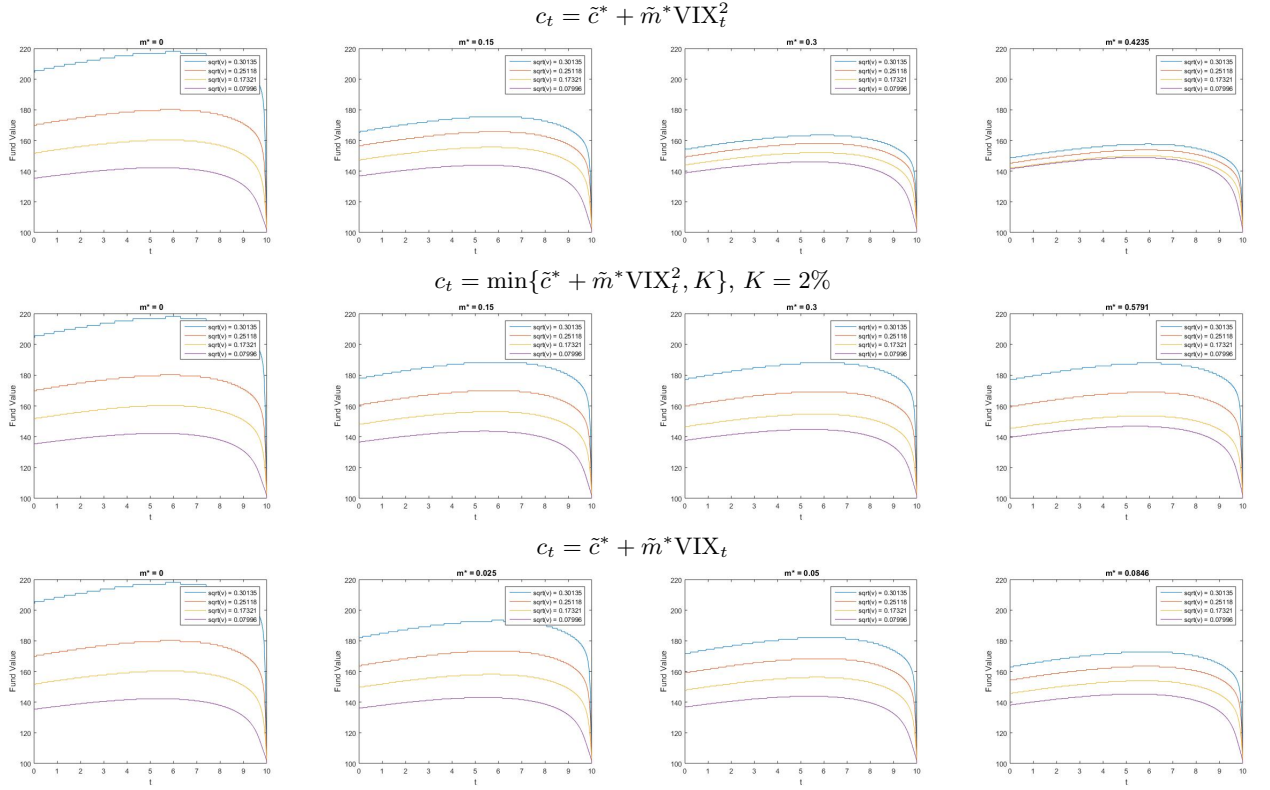


FIGURE 9. The y section of the approximated optimal surrender surface, $f_y^{(m,N)}$, for different volatility levels \sqrt{y} and fair multipliers \tilde{m}^* .

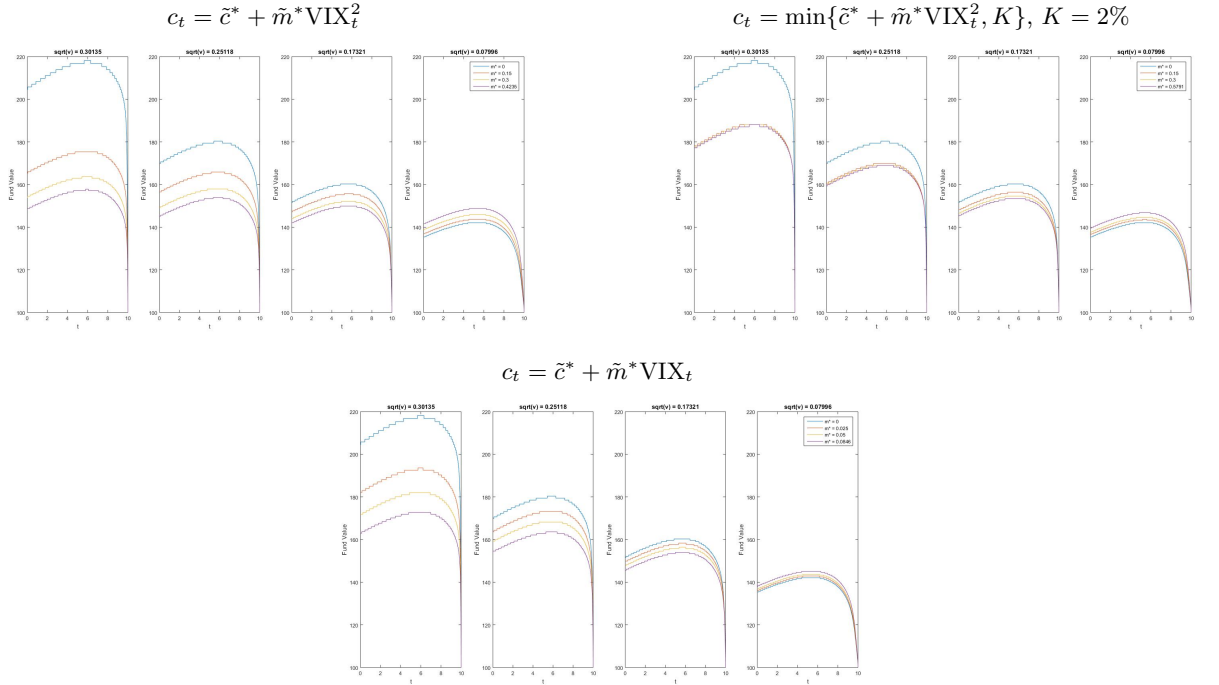


FIGURE 10. The y section of the approximated optimal surrender surface, $f_y^{(m,N)}$, for different volatility levels \sqrt{y} and fair multipliers \tilde{m}^* .